PIM1 KINASE IN ENDOTHELIAL CELL PROLIFERATION AND ADHESION

Dissertation

zur

Erlangung der naturwissenschaftlichen Doktorwürde

(Dr. sc. nat.)

vorgelegt der

Mathematisch-naturwissenschaftlichen Fakultät

der

Universität Zürich

von

Thomas Walpen

von

Binn VS

Promotionskomitee

Prof. Dr. Roland H. Wenger (Vorsitz)

Dr. Rok Humar (Leitung der Dissertation)

Prof. Dr. med. Edouard J. Battegay

Prof. Dr. Michael N. Hall

Zürich, 2012

1 TABLE OF CONTENTS

2 SUMMARY

PIM1 kinase (proviral insertion site for moloney leukemia virus 1) is expressed in different cell types, promoting cell growth, migration, differentiation and survival. This constitutively active serine-threonine kinase is mainly regulated at transcriptional and translational levels. As a proto-oncogene, PIM1 expression has been correlated with drug resistant tumors, tumor growth and cancer cell metastasis. It facilitates cell proliferation, migration and anti-adhesion.

Interactions between tumor cells and vascular endothelium are important for tumor growth. In the quiescent condition the endothelial monolayer provides a regulated barrier between the tissue and the blood stream. On the other hand sprouting from the endothelial monolayer is the initial starting point for the angiogenic process, which involves proliferation, migration and formation of endothelial tubes. Angiogensis is not only a prerequisite for tumor growth but also promotes and facilitates migration, invasion and metastatic spread of malignant cells.

Even though plenty of studies have investigated PIM1's function in cancer, little is known how PIM1 influences endothelial proliferation and so far there are no data on its contribution to barrier integrity of the endothelial monolayer.

In the first part of this thesis I have investigated, how PIM1 contributes to endothelial proliferation and whether it confers resistance to rapamycin-induced growth arrest. We found that *Pim1*$^{-/-}$ mouse aortic endothelial cell (MAEC) proliferation was significantly more sensitive to rapamycin, compared to wildtype cell growth rates. Interestingly, rapamycin treatment was accompanied with higher PIM1 protein levels in the cytosol and in the nucleus. Generation of an expression system consisting of *Pim1* c-terminal truncation mutants revealed a critical region responsible for nuclear localization of the protein. Truncations beyond a specific Serine, Serine 276, located to the nucleus, as also observed, when cells were treated with rapamycin. Reexpression of this mutant in *Pim1*$^{-/-}$ cells significantly increased proliferation. In summary we show, that nuclear PIM1 alone is sufficient to increase endothelial cell proliferation, which could explain the higher resistance of Pim1 wildtype cells to rapamycin.

In the second part of this thesis I have investigated if PIM1 also contributes to barrier integrity of the endothelial monolayer. *Pim1*$^{-/-}$ MAEC displayed decreased migration

in wound closure assays, slowed cell detachment after trypsinization and increased electrical resistance across the endothelial monolayer. Reintroduction of *Pim1*-cDNA into *Pim1*$^{-/-}$ MAEC significantly restored wildtype adhesive characteristics. *Pim1*$^{-/-}$ MAEC displayed enhanced focal adhesion and adherens junction structures as suggested by immunostainings for vinculin and β-catenin. Transcriptome analysis revealed junctional molecules such as *Cadherin 13* and matrix components such as *Collagen 6a3* to be highly upregulated in *Pim1*$^{-/-}$ cells. Intriguingly, extracellular matrix deposited by *Pim1*$^{-/-}$ cells alone was sufficient to induce the hyperadhesive phenotype in wildtype endothelial cells. Taken together these results show, that loss of *Pim1* induces a strong adhesive phenotype by enhancing endothelial cell-cell and cell-matrix adhesion by the deposition of a distinct extracellular matrix.

3 ZUSAMMENFASSUNG

Die Protein Kinase PIM1 (proviral insertion site for moloney leukemia virus 1) begünstigt in verschiedenen Zelltypen, Wachstum, Migration, sowie deren Fortbestand. Sie zählt zu den konstitutiv aktiven Kinasen und wird hauptsächlich auf transkriptioneller und translationeller Ebene reguliert. Eine hohe zelluläre *Pim1* Expression korreliert mit einer schnelleren Zellvermehrung, erhöhten Migrationsraten der einzelnen Zellen und einer Abnahme der Zelladhärenz, eine Eigenschaft die PIM1 zum Proto-Onkogen macht. Diese Faktoren erhöhen die Resistenz der Zelle gegenüber medikamentöser Behandlung und fördern Tumorwachstum und Metastasierung.

Wie schnell und ob überhaupt ein Tumor wächst, wird zu einem bedeutenden Teil durch das Wechselwirken von Tumorzellen und dem vaskulären Endothel bestimmt.

Im Ruhezustand fungiert das Endothel, bestehend aus einer einzigen Zellschicht, als Barriere zwischen dem Blutgefässsystem und dem Gewebe. Andererseits ist das aussprossen des Endothelzellschicht der Beginn der sogenannten Angiogenese. Bei diesem Prozess beginnen die Endothelzellen zu proliferieren und zu migrieren und bilden so neue Gefässe. Diese sogenannte Tumorangiogenese fördert jedoch nicht nur das Wachstum des kanzerösen Gewebes per se, sondern ermöglicht auch die Migration, die Invasion und die Metastasierung von malignen Zellen in die Peripherie und somit andere Organe des Körpers.

Obwohl schon viele Studien veröffentlicht wurden, die sich mit der Funktion der PIM1 Kinase in Tumoren befassen, ist eigentlich wenig bekannt darüber, wie PIM1 das endotheliale Zellwachstum ankurbelt und bis jetzt nichts, ob PIM1 die endotheliale Barrierefunktion beeinflusst.

Im ersten Teil dieser Studie habe ich mich zum einen mit der Frage befasst, wie PIM1 das Endothelzellwachstum beeinflusst und zum anderen ob es zudem eine gewisse Resistenz der Zellen gegenüber Rapamycin, einem Zellwachstumshemmer, hervorrufen kann. Wir explantierten Aorten aus Wildtyp und *Pim1*$^{-/-}$ Mäusen und extrahierten aus diesen Endothelzellen. Im Vergleich zu endothelialen Wildtyp Zellen, waren *Pim1*$^{-/-}$ Zellen bezüglich ihrer Wachstumsrate signifikant sensitiver gegenüber Rapamycin. Wir beobachteten, dass die Behandlung von Wildtypzellen mit Rapamycin zu einer grösseren Anzahl Zellen mit zytosolischem und nukleärem PIM1

führt. In der Folge entwickelten wir ein auf Plasmiden basierendes System zur Expression von *Pim1* in *Pim1*$^{-/-}$ Zellen. Wir verkürzten das c-terminale Ende der Pim1 Kinase schrittweise und exprimierten diese Konstrukte in *Pim1*$^{-/-}$ Zellen. Dadurch fanden wir heraus, dass das Fehlen des c-Terminus ab Serin 276 zu einer nukleären Lokalisation von PIM1 führt, wie wir das auch bei rapamycin behandelten Wildtyp Zellen beobachteten. Wird diese Mutante nun in *Pim1*$^{-/-}$ Zellen exprimiert, führt das zu einer signifikant höheren Wachstumsrate verglichen mit *Pim1*$^{-/-}$ Zellen die das ungekürzte, also das Wiltyp *Pim1* exprimieren. Zusammenfassend könnte man sagen, dass allein nukleäres PIM1 ausreicht um den endothelialen Zellwachstum zu erhöhen. Dies könnte auch die erhöhte Resistenz von Wildtyp Zellen gegenüber Rapamycin erklären.

Im zweiten Teil dieser Studie beschäftigte ich mich mit der Funktion, die PIM1 bei der Aufrechterhaltung der endothelialen Barriere einnimmt. Zellmigrationsexperimente zeigten, dass *Pim1*$^{-/-}$ Zellen erheblich langsamer migrieren und im Vergleich zu Wiltyp Zellen längere Inkubationszeiten mit Trypsin notwendig sind, um sie von der Kulturschalenoberfläche abzulösen. Zudem zeigten Messungen, dass ein *Pim1*$^{-/-}$ Zellrasen einen viel grösseren elektrischen Widerstand hat als dass dies bei Wildtyp Zellen zu beobachten ist. Wurde jedoch das fehlende PIM1 in *Pim1*$^{-/-}$ Zellen in Form einer *Pim1*-cDNA wieder zugegeben, wiesen die Zellen wiederum die adhesiven Eigenschaften des Wildtyps auf. Mit Immunfluoreszenzbildern konnten wir zeigen, dass Vinculin und β-catenin in *Pim1*$^{-/-}$ Zellen, Proteine die in focal adhesions und adherens junctions vorzufinden sind, ausgeprägtere Strukturen bilden. Wir fanden viel mehr Vinkulin in *Pim1*$^{-/-}$ Zellen vor und die β-catenin Färbungen in den adherens junctions waren viel länger als in den Wildtyp Zellen. Eine vergleichende Genexpressionsanalyse zeigte, dass tatsächlich viele Gentranskripte in *Pim1*$^{-/-}$ Zellen hochreguliert sind, die für Moleküle kodieren welche in die Zelladhäsion involviert sind. Unter anderem sind dies *Cdh13,* ein Protein der Zell junctions oder *Col6a3,* ein Protein der extrazellulären Matrix. Interessanterweise konnten wir letztlich zeigen, dass allein die von *Pim1*$^{-/-}$ Zellen ausgeschüttete Matrix genügt, um bei darauf wachsenden Wildtyp Zellen einen adhesiven Phänotypen zu induzieren.

Somit kann man sagen, dass das Fehlen von *Pim1* einen extrem adhesiven Phänotypen hervorruft. Dieser ist auf eine stärkere Zell-Zell, wie auch Zell-Matrix

Adhäsion zurückzuführen, die durch Sezernieren einer spezifischen Matrix hervorgerufen wird.

4 INTRODUCTION

4.1 Structure and functions of blood vessels

The circulatory system delivers essentials such as oxygen or nutrients to and carries waste products away from our organs and tissues. The functional units of this transportation system are the blood vessels, more precisely arteries, capillaries and veins, that altogether measure a stunning 50’000 km in length.

4.1.1 Assembly of the vessel wall

Three main layers composed of cells and matrix components form the vessel lumina of arteries and veins: the tunica externa, the tunica media and the tunica intima (Fig.1A).

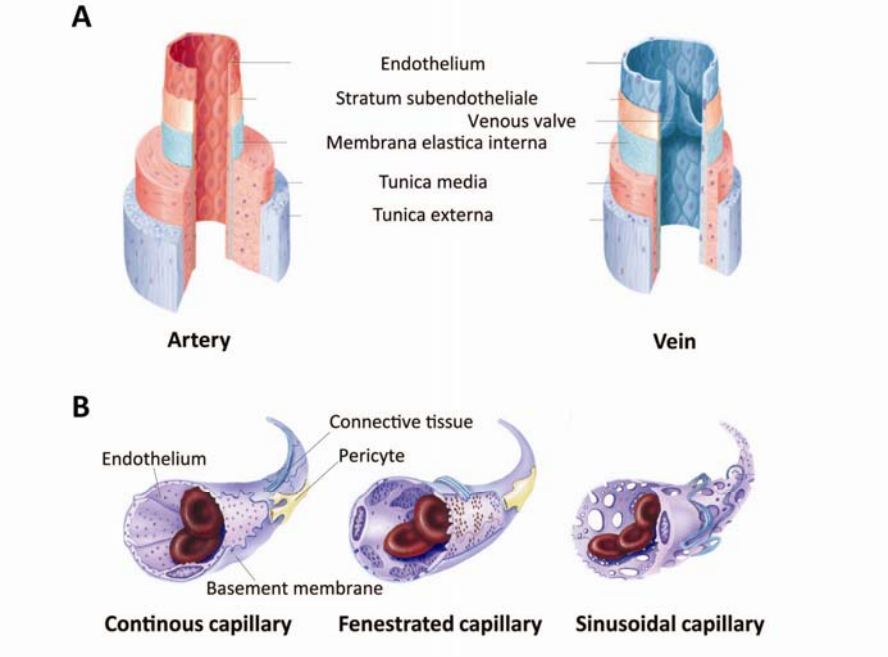

Figure 1. (A) Assembly of an arterial (left) and a venous (right) vessel wall. (B) Three different types of capillaries. A continous (left), a fenestrated (middle) and a sinusoidal capillary. Fig. 1A by Aumüller [3]; Fig. 1B adapted from Yale systems cell biology.

The outermost layer, the tunica externa or adventitia, contains connective tissue and is relatively thin in arteries or arterioles when compared to larger vessels: In the aorta, the adventitia contains small blood vessels, the vasa vasorum, that feed the larger vessel walls with nutrients. The second layer, the tunica media provides mechanical support against pulsatile blood flow. The tunica media is composed of smooth muscle cells embedded in a mesh of collagen and elastic fibers, that regulate blood flow through vasoconstriction and –dilation. The innermost layer facing the lumen is the tunica intima, composed by the stratum subendotheliale, which provides an anchoring basal lamina for a single layer of cells, the endothelium. Capillaries consist of a connected endothelium surrounded by a basement membrane and connective tissue, which is wrapped by pericytes (Fig.1B). Capillaries can be further divided into three types based on the morphology of the endothelial layer: Continuous, fenestrated and sinusoidal capillaries. The least permeable capillaries are characterized by a continuous endothelium. Fenestrated capillaries provide a continuous basement membrane, but manifest gaps between endothelial cells. The third type of capillaries, i.e., the sinusoids, are characterized by a discontinuous endothelium, exhibit large gaps in the endothelial monolayer and also a discontinuous basement membrane.

4.1.2 Endothelial barrier function

The endothelial monolayer serves as a highly regulated permeability barrier to ensure a controlled exchange of molecules through the vessel wall [11].

Two pathways ensure the controlled exchange between the vessel lumen and the interstitial space: The trans- and the paracellular pathway. In the resting endothelium transendothelial flux mainly occurs transcellularly [12]. This caveolae-mediated transcytosis from the vessel lumen through the cell to the interstitium is an important mechanism to maintain the fluid balance across the endothelial monolayer, the so-called oncotic pressure [13]. Mechanistically, binding of albumin to its receptor induces invagination of microdomains from the cell membrane. These so called caveolae separate as small vesicles into the cytoplasm and are able to fuse again with the basolateral site of the cell, discharging their cargo to the interstitial space of the vessel [14]. The paracellular pathway is pivotal in inflammation and cancer cell

extravasation [15]. Paracellular transport or paracytosis is regulated by interendothelial gap-, tight- and adherens junctions. Gap junctions serve as channels between the cells of the monolayer, to transfer water, ions and small molecules from cell to cell. However, tight- and adherens junctions not only restrict the paracellular flux, but also promote adhesion between adjacent cells [13]. Importantly, adherens junctions, beside their function as gatekeepers and cell adhesion proteins, may also regulate vascular homeostasis and contribute to cell proliferation, migration, and apoptosis via intracellular signaling cascades [16-18].

4.1.3 Adherens junctions and focal adhesions

Cadherins are the structural proteins of adherens junctions, connecting neighboring endothelial cells to one another. These single-pass transmembrane glycoproteins consist of an extracellular part, directly participating in adhesion, and a cytosolic domain that links to the cytoskeleton [19, 20]. Classical cadherins, such as VE-cadherin, the most prominent cadherin family member in endothelial cells, consist of extracellular cadherin (EC) domains. These ectodomain structures require calcium to mediate stability and orientation [21]. The ectodomains dimerize on the surface in order to bind to neighboring cells (Fig.2) [19]. The intracellular domain of cadherins interacts with the cytoskeleton through members of the catenin protein family: α-, β-, δ- (also known as plakoglobin) and χ-catenin (also known as p120) [22]. This complex regulates cell adhesion via intracellular signaling. As member of the canonical Wnt (wingless-int) signaling pathway, β-catenin also acts as a transcriptional co-factor in the nucleus. In tumorigenesis for example nuclear β-catenin leads to dissociation of the adherens junctions, and regulates proliferation and survival. [23, 24]. Plakoglobin, p120-catenin and β-catenin directly interact with cadherin, whereas α-catenin associates with plakoglobin and β-catenin providing a bridge to F-actin (filamentous actin) a major component of the cytoskeleton [25]. Structurally α-catenin provides binding sites for catenins and F-actin and is thought to stably wire the cytoskeleton and the adherens junction. However, recently α-catenin has been shown not to bind F-actin and β-catenin simultaneously [26].

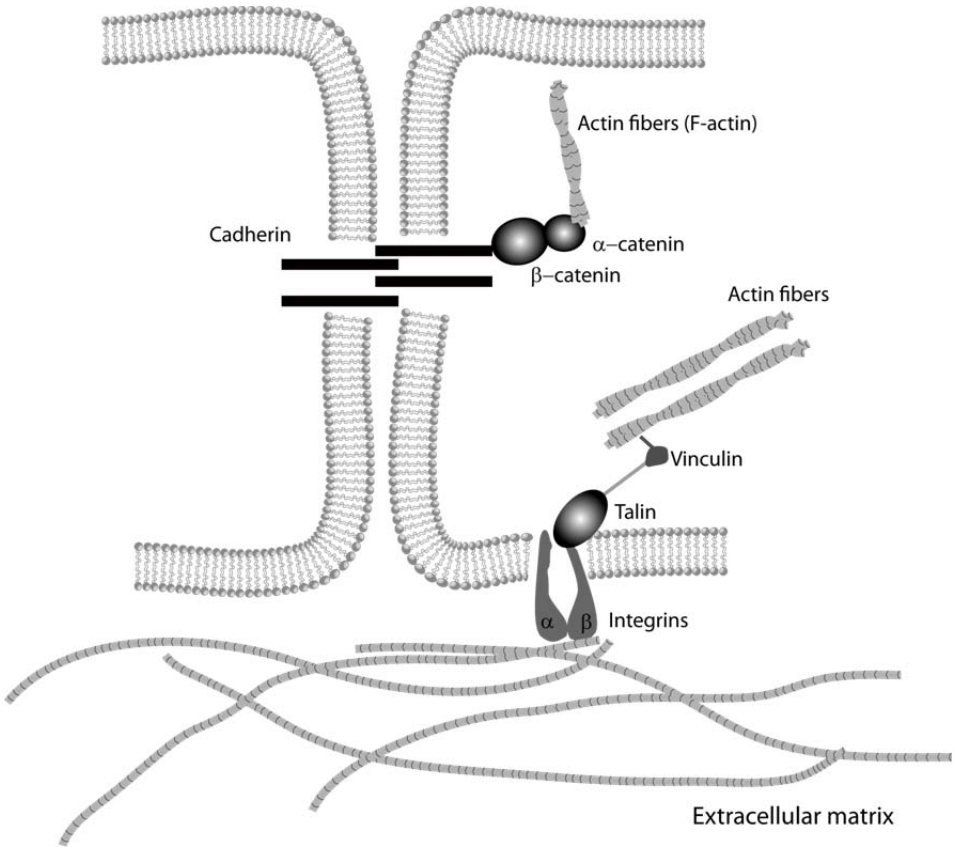

Figure 2. Simplified scheme of an adherens junction and a focal adhesion. Cell to cell contact is mediated through homophilic cadherin binding. Cadherin are then linked via catenins to the vytoskeleton. Cell to matrix contact is mediated via integrin receptors, which are connected to the cytoskeleton via Talin and vinculin.

Adhesion to the extracellular matrix (ECM) is mediated by a family of cell surface receptors, the integrins (Fig.2). Heterodimerization into α and β–integrin dimers confers the intrinsic substrate specificity, enabling the binding to different ligands such as collagens, laminins and other components of the ECM. Inside the cell, the intracellular part of the integrin receptor binds to talin, that links to the actin cytoskeleton via vinculin. Furthermore, the intracellular part of the integrin receptor interacts with focal adhesion kinase (FAK), which mediates signal transduction via different signaling pathways [27]. Integrin binding results in receptor clustering, actin reorganization and recruitment of signaling proteins to the membrane into focal adhesions [28]. Such focal adhesion clusters orchestrate cell migration, cell polarity and maintain cell growth and survival [29] whereby FAK mediates a dynamic crosstalk between focal adhesions and adherens junctions. [30].

4.2 Angiogenesis – a dynamic rearrangement of the endothelial barrier

In the adult, the tunica intima, i.e. the endothelial monolayer, remains quiescent. However, angiogenic factors can activate the endothelium in order to form new blood vessels from pre-existing ones, a morphogenic process known as angiogenesis [31]. Angiogenesis involves endothelial cell division, migration and sprout formation. This requires not only the disassembly and assembly of structural proteins at sites of endothelial adherens junctions and focal adhesions, but also dynamic changes of the endothelial cytoskeleton and the composition of the ECM. Figure 3 shows a model how new vessels are formed.

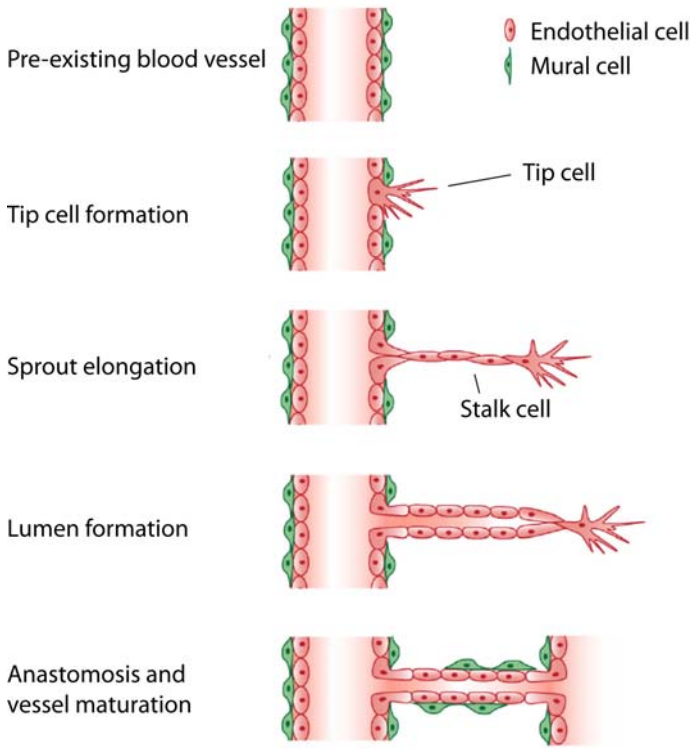

Figure 3. Schematic representation of the angiogenic process. Angiogenesis starts from pre-existing vessels, with the conversion of a previously quiescent endothelial cell into a tip cell. Tip cells form protrusions that invade the surrounding environment followed by a migrating column, of proliferating endothelial cells, the stalk cells. Within the stalk cells vacuoles form, which fuse and give rise to the vascular lumen. Upon formation, the new vessel is stabilized and matured mainly by reestablishment of intercellular adhesion and coverage with mural cells. Figure by Francavilla [7].

At the early onset of endothelial sprouting, endothelial cells are liberated of mural cells [32] and the basement membrane including the ECM through proteolytic cleavage [33]. Attracted by proangiogenic stimuli, endothelial tip cells start to protrude into the environment. Subsequently, stalk cells, following the leading tip, start to proliferate, to support sprout elongation and to form the new vessel lumen. Tip cells fuse with neighboring sprouts, a process known as anastomosis, to build a new vessel lumen. Finally, during vessel maturation, a new vascular basement membrane is deposited and mural cells, i.e., pericytes and vascular smooth muscle cells are recruited [34].

4.2.1 Tumor angiogenesis

Under physiological conditions angiogenesis occurs during wound healing, tissue repair and growth, and in the maternal uterine wall to establish the placental anchor [35]. Physiological angiogenesis turns into pathological vessel growth when the fine tuned control and negative feedback mechanism over angiogenic subprocesses are lost, become chaotic and unregulated [35]. In pathological situations blood vessel growth is either excessive, aberrant or insufficient. This is observed in highly prevalent diseases such as atherosclerosis, hypertension and cancer [36]. Figure 4A displays known mechanisms of tumor vessel growth [9]. Genetic, epigenetic and metabolic changes in cancer cells, key steps for cancer progression, can promote the 'angiogenic switch', the critical point when tumor vascularization is switched on. Furthermore, hypoxia, due to growth of tumors, is a main trigger for angiogenesis. Cells require oxygen and nutrients for their survival and are therefore located within 100 to 200 μm distance of blood vessels, the diffusion limit for oxygen [8]. Beyond a critical tumor volume, oxygen and nutrients will not diffuse to cells in the tumor core resulting in hypoxia. Hypoxia upregulates expression of hypoxia inducible transcription factors (HIFs) in the malignant cells, which then activate gene expression of proangiogenic stimuli (Fig. 5) [9]. Inhibitory molecules can furthermore keep the angiogenic balance to the "off" side. Many of these molecules derive from larger molecules with no intrinsic inhibitory potential. Upon proteolytic cleavage, the products, such as statins, unfold their antiangiogenic properties. In most tumors the angiogenic balance remains on the "on" mode, i.e. proangiogenic factors such as

VEGF (Vascular endothelial growth factor) or FGF (Fibroblast growth factor) predominate antiangiogenic factors (Fig 4B) [37].

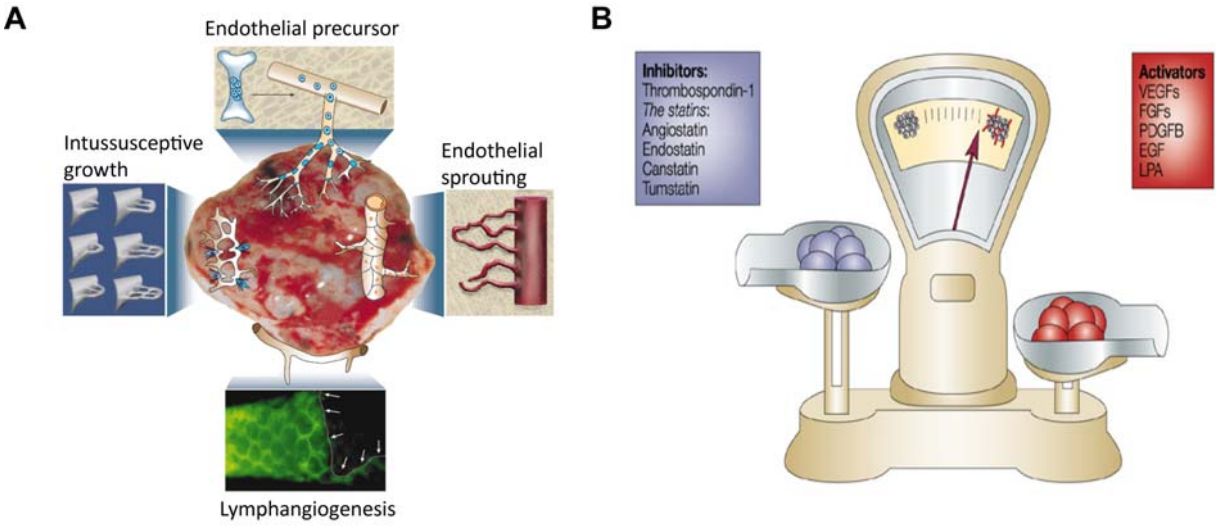

Figure 4. (A) Cellular mechanisms of tumor (lymph) angiogenesis. Tumor vessels grow by various mechanisms: (1) the host vascular network expands by budding of endothelial sprouts or formation of bridges (angiogenesis); (2) tumor vessels remodel and expand by the insertion of interstitial tissue columns into the lumen of pre-existing vessels (intussusception); and (3) endothelial cell precursors (angioblasts) home from the bone marrow or peripheral blood into tumors and contribute to the endothelial lining of tumor vessels (vasculogenesis). Lymphatic vessels around tumors drain the interstitial fluid and provide a gateway for metastasizing tumor cells. (B) Angiogenesis is orchestrated by a variety of activators and inhibitors. Activators of endothelial-cell proliferation are shown in the red box and inhibitors in the blue box. Figure by Carmeliet [9].

In contrast to physiologic blood vessel architecture, the vasculature in tumors is unorganized and highly chaotic. The blood vessels display dilated diameters with large variations in size, excessive vascular branching with disturbed and multidirectional blood flow [38]. Furthermore, cell-cell adhesion of the endothelial monolayer is decreased and the basement membrane incomplete or missing, resulting in leaky vessels [9]. This increase in vessel permeability enables tumor metastasis resulting in cancer cell extravasation into the circulatory system [39].

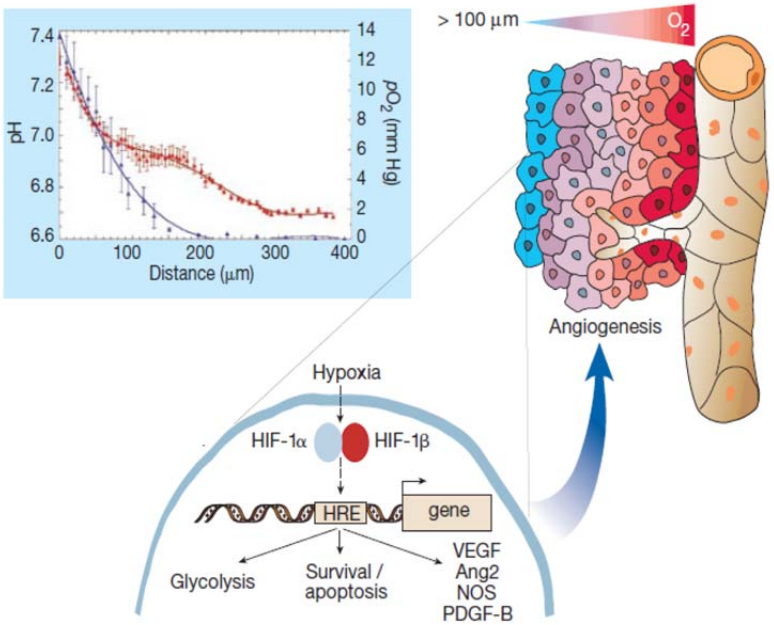

Figure 5. Because of the irregular pattern and organization of the tumor vasculature, some cells in tumors are located more than $100\mu m$ away from blood vessels and become hypoxic (red-to-blue gradient indicates progressive hypoxia). Tumor cells survive fluctuations in oxygen tensions, in part because clones are selected in hypoxic tumors that switch to a proangiogenic phenotype. HIFs increase transcription of several angiogenic genes and also affect cellular survival/apoptosis pathways. Box: relationship between the distance of tumor cells from nearby vessels and their degree of hypoxia (blue symbols) and acidosis (red symbols) Figure by Helmlinger [8]. Figure by Carmeliet [9].

4.3 TOR - the target of rapamycin

In the search for new antibiotics, the macrolid rapamycin, purified from a bacterial strain collected on the island of Rapa Nui (Easter island) was discovered in the 1960's, to have strong anti-proliferative and immunosuppressive effects in mammalian cells [40]. TOR1/2, the target of rapamycin in yeast, was identified thirty years later through mutational search for resistance to cell cycle inhibition by rapamycin in budding yeast [41]. The mammalian counterpart was found three years later by several groups independently, which is the reason that mammalian target of rapamycin (mTOR) is also known as FKBP12-rapamcyin-associated protein (FRAP),

rapamycin and FKBP12 target (RAFT), rapamycin target (RAPT), or sirolimus effector protein (SEP) [42-46].

4.3.1 mTOR complex 1 and mTOR complex 2

mTOR contains a serine/threonine protein kinase domain and exists in two multiprotein complexes mTORC1 (mTOR complex 1) and mTORC2 (mTOR complex 2) (Fig.6). Formation of mTORC1 requires assembly of raptor (regulatory associated protein of mTOR), PRAS40 (Pro-rich Akt substrate) and deptor (DEP domain-containing mTOR-interacting protein), mLST8/GβL (mammalian lethal with SEC13 protein 8 /G-protein β-subunit like protein) into the complex. mLST8/GβL is also a component of mTORC2 and appears to be more critical for mTORC2 function [47, 48]. Besides mLST8 and deptor mTORC2 further requires mSIN1 (mammalian stress-activated map kinase-interacting protein 1), PROTOR (protein observed with rictor) and rictor (rapamycin-insensitive companion of mTOR) [48, 49] as components for proper function. Rapamycin bound to FKBP12 (FK506-binding protein) effectively and rapidly inhibits mTORC1. mTORC2 is not acutely inhibited by rapamycin, however long-term or high-dose treatment also affects mTORC2 assembly [50].

4.3.2 The mTOR pathway

The mTOR pathway is a central regulator of cell growth and proliferation, but also regulates cell survival, motility and metabolism. mTOR integrates different signals and functions [51]. Four major inputs have been implicated in mTOR signaling: growth factors, energy, nutrients and stress [52] (Fig.6).
mTORC1 integrates signals from stress, energy, growth factors and amino acids to promote cell growth, protein synthesis, cell proliferation and cell metabolism [53, 54]. With the exception of amino acids, all other signals modulate the activity of the TSC1-TSC2 (tuberous sclerosis complex1/2) complex, which negatively regulates mTORC1. By blocking TSC1/2 activity, growth promoting signals activate mTOR signaling, whereas stress signals inactivate the mTOR cascade. The two major downstream kinase targets of mTORC1 are S6K (ribosomal S6 protein kinase 1) and

4EBP (eukaryotic initiation factor (eIF) 4E-binding protein 1), contributing to cell growth (protein synthesis) and cell cyle progression [4, 48]. Activated mTORC1 also triggers a negative feedback loop via S6K: Activated S6K phosphorylates insulin receptor substrate 1 (IRS-1), leading to its proteasomal degradation and partial inhibition of PI3K/AKT signalling [55].

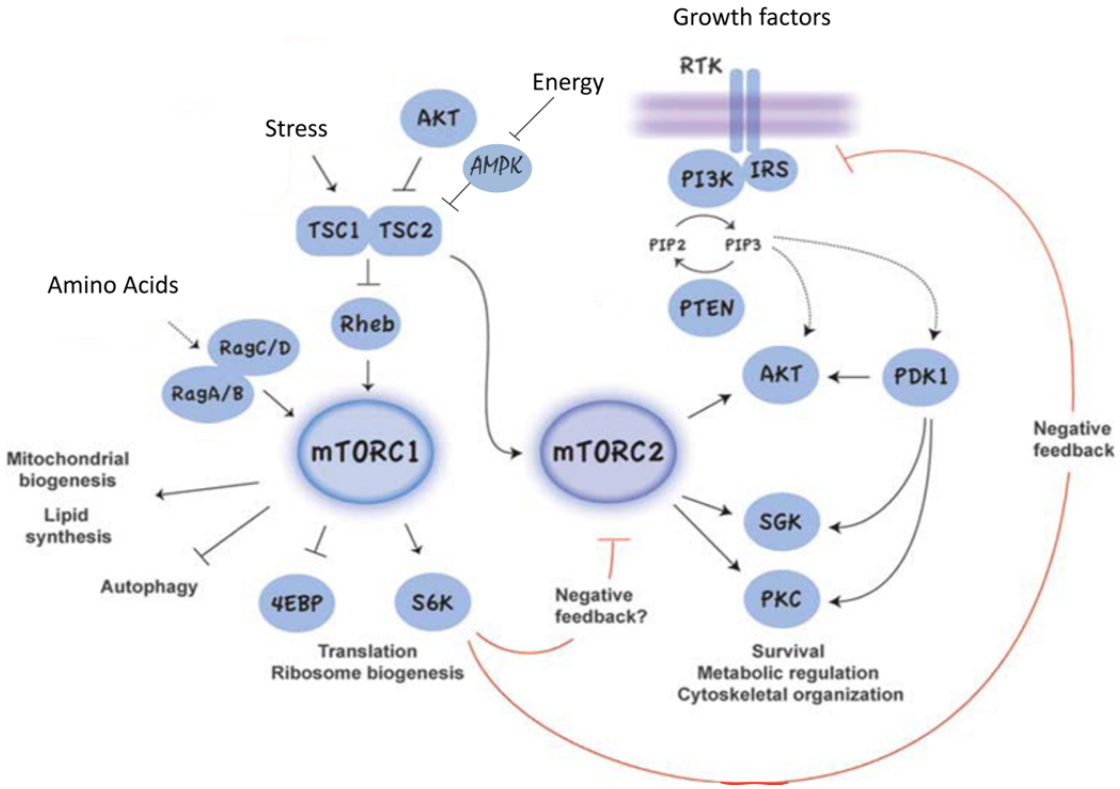

Figure 6. Simplified representation of mTOR signalling. mTORC1 and mTORC2 integrate extracellular inputs such as energy, stress, nutrients and growth factors, to regulate cell growth, proliferation and survival. Figure adapted from Foster [4].

AKT/PKB (protein kinase B) is a protein downstream of PI3K signalling. Upon growth factor signaling AKT is phosphorylated by PDK1 (phosphoinositide-dependent kinase 1), which is facilitated by mTORC2 activity. Complete activation of AKT requires additional phosphorylation of AKT on Ser473 by mTORC2. [56]. However upstream regulators of mTORC2 are largely unknown. Recent data suggest that mTORC2 activity requires association with ribosomes promoted by PI3K [57]. Finally, mTORC2

activity affects several cellular processes such as cell proliferation, cell survival, and organization of the actin cytoskeleton [58].

Thus, the mTOR pathway regulates many major cellular processes and is implicated in an increasing number of pathological conditions, including cancer, obesity, type 2 diabetes, and neurodegeneration.

4.4 PIM1 and the family of PIM kinases

PIM1 is a constitutively active serine threonine kinase [59] discovered as a proviral integration site for moloney murine leukemia viruses. The family of PIM kinases consists of three members PIM1, 2 and 3 (Fig.7) [60-62].

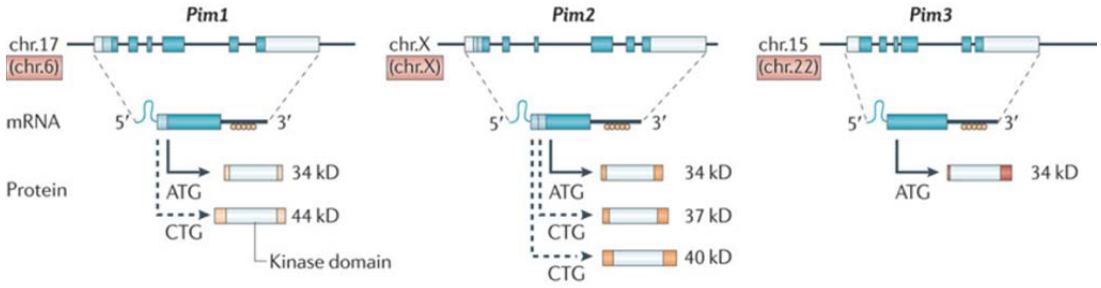

Figure 7. *Pim* genes are located at different chromosomal locations in the mouse and human genome, as indicated by black numbers and numbers in orange boxes, respectively. *Pim* mRNA transcripts are encoded by 6 exons (dark blue boxes) with large 5′ and 3′ untranslated regions (UTRs; white boxes) containing a G/C-rich region (light blue lariat) and five copies of AUUUA destabilizing motifs (orange circles), respectively [1]. Different protein isoforms are synthesized using alternative translation initiation sites (solid and dashed arrows) and additional codons present at the 5′ of these mRNAs are depicted as light blue boxes. PIM protein isoforms have different molecular masses but retain their serine/threonine kinase activity [2]. Pim kinases have no regulatory domains and their highly conserved kinase domain is indicated by a white box. Figure by Nawjin [10].

PIM kinases are highly conserved between species, share high homology to each other and exert complementary functions [1, 62]. Mice deficient for all three *Pim* kinases displayed reduced body size and impaired responses to hematopoietic growth factors, but were viable and fertile [1]. This finding suggests that PIM kinases,

including PIM1, are important but dispensable factors for growth factor signaling. Therefore, PIM kinases, which have proto-oncogenic activity, also emerged to interesting targets in cancer therapy (see section 4.4.1). In healthy conditions PIM kinases are expressed at low levels and in different cell lineages, such as hematopoietic cells, cardiomyocytes or vascular smooth muscle cells [63-65]. In endothelial cells PIM1 is transiently expressed during in vivo angiogenesis and induced by Vascular endothelial growth factor (VEGF) in human umbilical vein endothelial cells (HUVECs). Furthermore, PIM1 silencing impaired vascular endothelial growth factor-A (VEGF-A)-induced proliferation and migration and inhibited capillary formation on matrigel and endothelial cell sprouting in HUVECs [66].

PIM1 is involved in several signal transduction pathways (see section 4.4.1). Many different cytokines activate *Pim1* expression through growth factor signaling pathways, like the Janus kinase and signal transducer and activator of transcription (JAK–STAT) pathway [67, 68]. Due to its anti-apoptotic activity PIM1 is referred to as a proto-oncogene involved in the progression of different cancer types.

4.4.1 The Pim1 oncogene

PIM1 kinase expression is increased in different tumours from epithelial and haemotopoetic origin [10]. In most haematopoetic malignancies PIM1 expression correlates with a poor prognosis [69, 70], however in pancreatic non-small-cell lung cancer and in pancreatic ductal carcinoma PIM1 expression inversely correlated with prognosis [71, 72]. Elevated *Pim1* mRNA and protein levels correlate with the metastatic potential of tumors by facilitating migration and anti-adhesion as shown in tongue squamous cell carcinoma [73], gastric cancer [74] and in lymph node metastasis [75]. Vice versa, inhibition of PIM1 kinase activity diminished cancer cell migration and invasion in vitro [75].

Since the discovery of *Pim1* as a proviral insertion of moloney leukemia virus several different modes of action have been shown of how PIM1 contributes to tumorigenesis (Fig.8): PIM1 promotes cell growth, migration, differentiation and survival through phosphorylation of different substrates [76]. PIM1 promotes cell cycle progression by phosphorylation of the cell cycle inhibitors $p27^{Kip1}$ and $p21^{Cip1/WAF1}$ [77, 78]. $p27^{Kip1}$

phosphorylation induced cytoplasmic localization and subsequent proteasomal degradation of cycline-dependent-kinase inhibitor. $p21^{Cip1/WAF1}$ also localized to the cytoplasm once phosphorylated by PIM1 kinase. Another substrate of PIM1 is the protein kinase Cdc25 C-associated kinase 1 (C-TAK1). The phosphorylation of C-TAK1 significantly decreased its ability to phosphorylate and inactivate Cdc25C, a protein that promotes cell cycle progression [79]. Suppressor of cytokine signalling (SOCS) proteins are essential for T-cell differentiation. PIM1 physically interacts with SOCS family members and potentiates

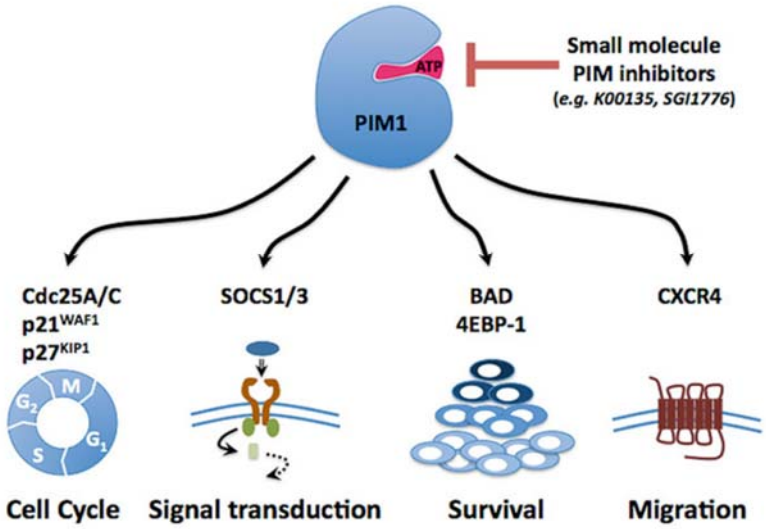

Figure 8. Different phosphorylation targets of PIM1 signalling and their functional outcome. In red the ATP binding pocket, which is the target for small molecule PIM1 kinase inhibitors. Figure by Stavropoulou [5].

their inhibitory effect on STAT5 mediated transcription [80]. Another PIM1 substrate is the pro-apoptotic protein B-cell-lymphoma-2-antagonist of cell death (BAD). PIM1 was found to phosphorylate BAD on serine 112, a gatekeeper site for its inactivation. This suggests a possible mechanism for PIM1 to enhance Bcl-2 activity and thereby to promote cell survival [81]. Furthermore, PIM1 was found to be a regulator of CXCL12-CXCR4-mediated homing and migration of hematopoietic stem cells. Bone marrow cells from *Pim1*$^{-/-}$ expressed less CXC-Motive-Chemokinereceptor 4

(CXCR4) and PIM1 activity was essential for cell migration towards a CXCL12 gradient [82].

PIM1 contains an ATP binding pocket as usual for protein kinases, however PIM1 is kinase is active without phosphorylation. Nevertheless, in the past several PIM1 kinase inhibitors emerged, binding to this cavity, with in vivo and vitro anti-cancer activity [76].

4.4.2 PIM kinases and mTOR signalling

The PIM and the mTOR/AKT pathway integrate growth factor signalling and promote cell proliferation and survival [10, 52]. They both share phosphorylation targets such as BAD or eukaryotic translation-initiation factor 4E (EIF4E) (Fig.9).

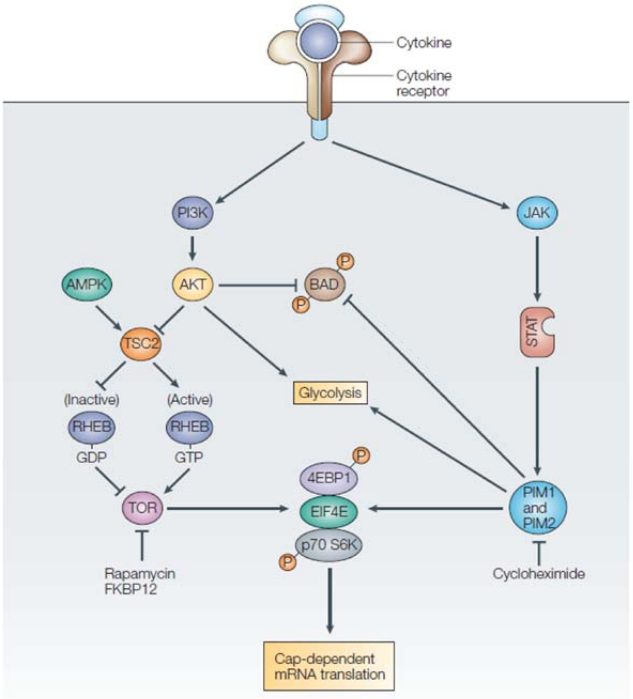

Figure 9. Growth-factor receptors that promote cell survival also activate members of the JAK and STAT family, resulting in the transcription of a set of genes, including those encoding the kinases PIM1 and PIM2. The AKT and TOR pathway and the PIM1 and PIM2 pathway function as overlapping, but functionally distinct, regulators of key metabolic pathways. Similar to TOR, PIM2 regulates key effectors of cap-dependent translational initiation, including EIF4E, the translational repressor EIF4E-binding protein 1 (4EBP1), and p70 S6 kinase (p70 S6K). Figure by Fox [6].

Furthermore it has been shown that *Pim1* depletion decreased the potential of AKT mediated survival signaling. In the myocardium of mice PIM1 expression increased after acute pathological injury and was also elevated in failing hearts of both mice and humans. Cardioprotective stimuli associated with AKT activation induced PIM1 expression, but could not protect the myocardium in *Pim1*$^{-/-}$ mice [65]. PIM kinases also appear to mediate drug resistance to rapamycin. While it has a minimal effect on T cell expansion in vitro and in vivo, cells from *Pim1*$^{-/-}$ *Pim2*$^{-/-}$ animals displayed an unexpected sensitivity to rapamycin [83]. In animal lymphoma models pharmacological blockade of the translation initiation complex was highly effective against converging signals of AKT and PIM kinases [84]. Additionally, PIM1 has been suggested to increase mTOR activity through phosphorylation of PRAS40 in Factor-Dependent Cell Progenitor cells (FDCP cells) [85]. Thus the PIM and the mTOR pathway seem to have overlapping functions, which can partially substitute for each other.

5 MATERIALS AND METHODS

5.1 Cell culture & transfection

MAECs were isolated from aortae of FVB/N wildtype and *Pim1*$^{-/-}$ mouse strains as described previously [86]. For all experiments cell culture dishes were precoated with 0.1% gelatine gold (Carl Roth GmbH, Karlsruhe, Germany) for 20 minutes at 37°C. Cells were maintained in DMEM (Biochrom, Berlin, Germany) complemented with 10% FBS, 1% sodium pyruvate, 1% non-essential amino acids and 1% penicillin-streptomycin (Invitrogen, LuBioScience GmbH, Luzern, Switzerland). Cell numbers were assessed with a NucleoCounter® NC-100™ (Chemometec, Allerød, Denmark). In all experiments ~ 8×10^4 cells/cm^2 were seeded, washed with phosphate-buffered saline (PBS) (Invitrogen, Carlsbad, CA) after 24 hours and trypsinized (TripLE express, Invitrogen, Carlsbad, CA) for further processing. The percentage of adherent cells was calculated as follows: [Total cell count – detached cell count]/Total cell count. Light micrographic pictures were acquired using an IX71 inverted microscope (Olympus, Volketswil, Switzerland). Compound K00486 was applied at a concentration of 100nM to wildtype cells. For PIM1 overexpression human cDNA encoding PIM1 was subcloned into a pCMV-Tag2A or a pdsRED C1 expression vector (kind gift of Jürg Schwaller, Department of Biomedicine, University Hospital, Basel, Switzerland) and cell transfection was performed with 50ng of vector/reaction using a basic endothelial cells nucleofector kit in a Nucleofector II device (Amaxa Biosystems, Cologne, Germany) according to the manufacturers protocol.

5.2 Wound healing assay

Pim1 wildtype and knockout MAEC were grown to confluency in 6-well plates and wounded with a 200 μl pipette tip along a ruler. Wounded monolayers were washed three times with growth medium before further incubation. At the indicated time points (0, 4, 8 and 24 hours), monolayers were photographed 3 times for each well at 20x magnification. Wound width was measured on hard copy prints of the images. Individual cell paths were determined for leading-edge cells along five uniformly

spaced lines along the wound edge. Initial wound at 0 hours was defined as 0% wound closed, total closure was defined as 100% wound closed.

5.3 Matrix exchange experiment

~ 8×10^4 cells/cm^2 wildtype and *Pim1*$^{-/-}$ MAECs were grown on 6-well plates (BD Biosciences, Franklin Lakes, NJ) for 24 hours. The cells were lysed with 25mM ammoniumhydroxyde (Sigma-Aldrich, St. Louis, MO) in PBS while leaving the extracellular matrix (ECM) intact. Wildtype cells grown on wildtype or *Pim1*$^{-/-}$ ECM for 24 hours were then trypsinized for 1, 2 or 3 minutes. To collect all the cells at each time point the cell layers were washed 3 times with PBS and the cell numbers in the collected supernatants were assessed and percentage of adherent cells was calculated as described above.

5.4 Immunoblotting

Total cell lysates were prepared using RIPA buffer as described before [87]. After SDS-PAGE, proteins were transferred onto polyvinylidene fluoride (PVDF) membrane (Millipore, Billerica, MA). The membrane was blocked with 4% skim milk powder in TBS-Tween solution or 4% BSA and probed with following antibodies: rabbit polyclonal anti-PIM1 (Cell Signaling Technology, Danvers, MA), primary mouse monoclonal to vinculin (abcam, Cambridge, MA), rabbit polyclonal anti-β-catenin (Cell Signalling Technology, Danvers, MA), rabbit polyclonal anti-α-Tubulin (Cell Signalling Technology, Danvers, MA), rabbit polyclonal anti-Histone H3 (Cell Signalling Technology, Danvers, MA), rabbit polyclonal anti-T-cadherin (Sigma-Aldrich, St. Louis, MO), rabbit polyclonal anti-COL6A3 (Abnova Coorporation, Neihu, Taipei), mouse monoclonal anti-FLAG (Sigma-Aldrich, St. Louis, MO) and mouse monoclonal anti-β-actin (Sigma-Aldrich, St. Louis, MO). Anti-mouse or rabbit-HRP-conjugated IgGs (Cell Signalling Technology, Danvers, MA) were used for visualization of relevant proteins on X-ray films by a chemiluminescence reaction (Thermo Scientific, Waltham, MA).

5.5 Fluorescence imaging

The cells were fixed in 4% paraformaldehyde for 20 minutes at 37°C on coverslips (Karl Hecht AG, Sondheim, Germany) and then permeabilized with 0.5% Triton X-100 in PBS for 10 min. After blocking for 45 minutes with goat serum the cells were incubated with the following antibodies: mouse monoclonal to PIM1 (Santa Cruz, Santa Cruz, CA), mouse monoclonal to vinculin (abcam, Cambridge, England), rabbit polyclonal anti-β-catenin (Cell Signalling Technology, Danvers, MA), mouse monoclonal anti-FLAG (Sigma-Aldrich, St. Louis, MO) and rabbit polyclonal COL6A3 antibody (Abnova Coorporation, Neihu, Taipei). After 3 washing steps cells were incubated with Alexa Fluor 555-conjugated secondary antibody (Invitrogen). F-actin was probed with Alexa Fluor 488 phalloidin and the nuclei were stained with Hoechst 33342 (Invitrogen). The coverslips were then mounted with FluorSave™ (Merck, Darmstadt, Germany) on glass slides (Thermo Scientific, Waltham, MA). Fluorescence imaging was performed using a ZEISS Axioskop fluorescence microscope (Carl Zeiss AG, Oberkochen, Germany) and a confocal laser scanning microscope Leica SP5 (Leica, Wetzlar, Germany).

5.6 qRT-PCR

RNA was isolated using a RNAeasy Mini kit (Qiagen, Hilden, Germany), followed by a on column DNA digestion (Qiagen, Hilden, Germany). cDNA was transcribed from total RNA using Omniscript RT kit (Qiagen, Hilden, Germany) and random primers (Roche, Basel, Switzerland). To control for DNA contamination in the qRT-PCR, for each sample a control reaction missing reverse transcriptase was additionally amplified. Primers for microarray validation and genotyping wildtype and *Pim1*$^{-/-}$ cells (supplementary material table S1, section 13) were designed using Primer3 software (http://frodo.wi.mit.edu/primer3). Primers for validation were tested by cDNA dilution series to obtain optimal reaction conditions. qRT-PCR was performed using an iCycler iQ Real Time PCR Detection System (Biorad, Reinach, Switzerland) and iQ™ SYBR® Green Supermix (Biorad). 250ng cDNA/reaction was amplified using indicated primers (Table S1) in duplicates in a final reaction volume of 25μl. Each representative reaction was loaded on an agarose gel for amplicon length analysis

and additionally the melting curve was analyzed. The qRT-PCR was quantified as follows: $2^{-\Delta C}{}_T$ = C_T gene of interest – C_T *gapdh* [88].

5.7 Electric cell-substrate impedance sensing

Resistance measurements were performed using an ECIS ZΘ apparatus (Applied Biopyhysics Inc.,Troy, NY) and either 8W1E arrays (Fig.20) or 8W10E+ arrays (Fig. 18, 21) both consisting of 8-wells with an area of 0.8 cm^2/well each and 1 or 40 gold electrodes with a diameter of 250 µm, respectively (Applied Biopyhysics Inc., Troy, NY). Before seeding cells, each well was preincubated with serum-free DMEM overnight followed by a 20 minutes coating with 0.1% gelatine gold (Carl Roth GmbH, Karlsruhe, Germany) and 0.9% sodium chloride in PBS, followed by 3 wash steps with serum free DMEM. 17 hours post transfection cells seeded into 8W1E and 8W10E+ plates, respectively. The arrays in the measurement station were then placed in an incubator (37°C, 5% CO2). Total resistance was measured in real-time at a frequency of 4 kHz. The complex impedance spectrum (Z, R, C) for each well was measured by applying an AC signal to the cells on the gold electrode, which output is measured over a frequency spectrum from 62.5 Hz to 64 kHz every 180 seconds by a second counter electrode. From this data the α^2.[$\Omega \times cm^2$] value and R_b [$\Omega \times cm^2$] was calculated using ECIS software (Applied Biopyhysics Inc.Troy, NY).

5.8 Cloning

Full length Pim1 was inserted into pCMV-Tag 2A by restriction enzyme digest from pdsRED with EcorI/SalI. The *Pim1* truncation constructs were amplified from a pdsRED C1-*Pim1* vector with specific primers, containing the restriction sites BglII/SalI and subcloned into pCMV-Tag 2A and pdsRED C1 vector system (for details see section 8.5). pPCR amplifications were performed using the PfuTurbo® DNA-polymerase (Stratagene, La Jolla, CA). The primers are listed in the primer table (supplementary material table S2, section 12).

5.9 Proliferation assay

4×10^3 MAEC/well were plated in 96-well cell culture dishes (TPP, Trasadingen, Switzerland) o/n. Cells were washed three times with PBS and 24 hours starved in DMEM without FCS. Then rapamycin or diluent was added for 1 hour and subsequently FCS was added to the cells cultures in a final dilution of 10%. Proliferation was measured with the metabolic indicator Alamar blue (Invitrogen, Carlsbad, CA), which was added at 24–48 h after rapamycin treatment. The degree of proliferation was determined using SpectraMax microplate reader (Molecular Devices, Sunnyvale, CA), applying an excitation wavelength from 530nM and an emission wavelength of 590nm. Control wells contained DMEM with appropiate rapamycin concentrations to provide a background level measurement.

5.10 Kinase inhibitors and extraction of cytosolic and nuclear fractions

To inhibit protein kinases of different signalling pathways, the cells were seeded and grown overnight, as described in cell culture methods. Afterwards the cells were washed three times with PBS and 24 hours starved in DMEM without FCS. Then the appropriate inhibitor or diluent was added for 1 hour and subsequently FCS was added to the cells cultures in a final dilution of 10%. After 3 hours the cells were harvested and cytosolic and nuclear fractionation was performed with a NE-PER nuclear and cytoplasmic extraction kit (Thermo Scientific, Waltham, MA), according to the manufacturers protocol.

Inhibitor	Target protein	Abbreviation	Concentration
Akt inhibitor IV	AKT/Protein kinase B	AKT	1μM
$Gö_{6983}$	Protein kinase C α,β,λ,δ,ζ	PKC	1μM
U_{0126}	Mitogen-activated protein kinase 1/2	MEK	5μM
$GSK3_{IX}$	Glycogen synthase kinase-3 α/β	GSK	1μM
Rapamycin	Mammalian target of rapamycin	RPM	0.25μM
LY_{294002}	PI3Kinase	LY	5μM

Table 1. List of the different kinase inhibitors with their corresponding target and the final concentration used.

5.11 FACS analysis

The apoptosis assay was performed using a Fluoresceinisothiocyanat (FITC) Annexin V/Dead cell apoptosis kit (Invitrogen, Carlsbad, Ca). Therefor the cells were harvested and washed in cold PBS. After centrifugation the cells were resuspended in 1X annexin-binding buffer to a density of ~1×10^6 cells/mL. According to the protocol 5μl of FITC Annexin V and 1μl of the 100μg/mL Propidium iodide (PI) working solution were added to each 100μl of cell suspension. After 15min incubation at room temperature, 400μl of 1X annexin-binding buffer was added to each sample and the tubes were kept on ice until sorting. The samples were then analyzed with a FACSCalibur (Becton Dickinson, Franklin Lakes, NJ) at emission wave lengths of 530nm and >575nm.

5.12 Statistical analysis

All statistical tests were performed using GraphPad Prism 5.04 for Windows (GraphPad software, San Diego, CA). For analysis of repeated measurements a two way Anova followed by a Bonferroni post test was performed. Differences between two groups were evaluated using unpaired t-test. To compare more than two groups one way anova followed by a Bonferroni post test was done. a.u.c. was calculated over indicated time periods using GraphPad software. Data are represented as means ± s.e.m.

6 RATIONALE AND AIMS OF THE 1ST PART OF THE THESIS

In the past years many studies on rapamycin and its effect in cancer therapy have been performed. However, the inhibitory effects on tumor growth remain restricted to specific cancer subtypes and have not a generally extended efficacy. This drug resistance can be caused by redundant signalling pathways. In the past, several proteins have been identified, which counteract rapamycin-induced growth arrest . Therefore, these molecules may serve as targets for combined drug therapy, to improve the efficacy of anti-cancer treatments. PIM kinases have been shown to substitute for mTOR-mediated signalling. Combination of PIM1 kinase inhibitors and rapamycin may have a beneficial effect on regression of tumors. Nevertheless, tumor growth depends highly on vessel infiltration into the malignant tissue. Therefore, in addition to blocking cancer cell growth, inhibition of tumor angiogenesis may be of relevance. PIM1 has been described in various human tumors. Yet little is known about the function of PIM1 in relation to mTOR signalling on endothelial cells.

One goal of my thesis was:

- To explore whether abrogation of PIM1 improves known growth inhibitory effects of rapamycin on endothelial cells and if so…

- To investigate the mechanisms by which PIM1 antagonizes the antiproliferative properties of rapamycin.

7 RESULTS PART I :

PIM1 nuclear translocation confers rapamycin insensitivity in endothelial cells and promotes cell proliferation

7.1 *Pim1* deletion enhances the inhibitory effect of rapamycin on cell proliferation.

T-cells deficient for *Pim1* and *Pim2* displayed an unexpected sensitivity to rapamycin. The cellular response to rapamycin was not only restricted to a decrease in survival, but also to complete abrogation of proliferation [83]. Based on this observation we investigated whether *Pim1* deletion similarly affects the proliferative response in endothelial cells.

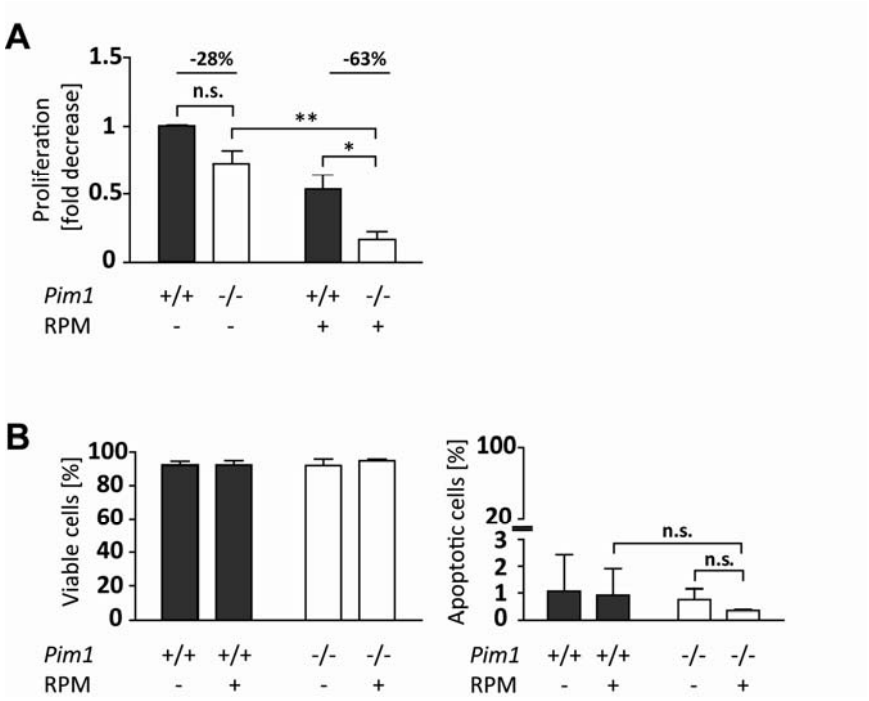

Figure 10. Cell proliferation and apoptosis of wildtype vs. *Pim1*$^{-/-}$ endothelial cells. (A) Fold decrease cell proliferation of wildtype compared to *Pim1*$^{-/-}$ MAEC treated with 250nM rapamycin (RPM) and control. (B) FACS analysis of corresponding treatment conditions of wildtype vs. *Pim1*$^{-/-}$ cells. Wildtype cells (black bars), *Pim1*$^{-/-}$ cells (white bars). Data are represented as means ± s.e.m. (n=3). **P*<0.05, ***P*<0.01

Wildtype and *Pim1*$^{-/-}$ endothelial cells were treated for 24 hours with and without rapamycin (RPM). Proliferation, viability and apoptosis were quantified (Fig. 10). *Pim1* knockout decreased proliferation by 28 ± 0.1% compared to wildtype cells (Fig. 10A left side). *Pim1* knockout MAEC treated with rapamycin reduced proliferation by 63 ± 0.1% in comparison to wildtype cells (Fig. 10A right side). Thus, we found a 1.3-fold and a 3.2-fold decrease in proliferation after rapamycin treatment in wildtype and knockout cells, respectively. To exclude a possible toxic effect of rapamycin resulting in reduced cell numbers due to apoptosis, we analyzed cell viability by FACS analysis (Fig. 10B). Wildtype and *Pim1*$^{-/-}$ cells grown under the same conditions were sorted by FACS. We observed no decrease in the percentage of viable wildtype or *Pim1*$^{-/-}$ cells after rapamycin treatment (Fig. 10B left panel). Under all conditions more than 90% cells were viable. Accordingly, no significant increase of the apoptotic cell population was observed, comparing wildtype and *Pim1*$^{-/-}$ cells treated with rapamycin and controls (Fig. 10B right panel). In all conditions tested the percentage of apoptotic cells was less than 2%. Taken together, these data suggest, that *Pim1* knockout in endothelial cells increases sensitivity to rapamycin.

7.2 mTOR and Akt inhibition increases PIM1 protein expression.

To investigate whether mTOR inhibition by rapamycin and subsequent changes in cell proliferation specifically affect PIM1 protein levels, we treated wildtype MAECs with protein kinase inhibitors blocking different signaling cascades (Table 2).

Inhibitor	**Target protein**	**Abbreviation**
Akt inhibitor IV	AKT/Protein kinase B	Akt
$Gö_{6983}$	Protein kinase C α,β,λ,δ,ζ	PKC
U_{0126}	Mitogen-activated protein kinase 1/2	MEK
$GSK3_{IX}$	Glycogen synthase kinase-3 α/β	GSK
Rapamycin	Mammalian target of rapamycin	RPM
LY_{294002}	PI3Kinase	LY

Table 2. Compounds used to inhibit different signalling cascades.

We furthermore differentiated between cytosolic and nuclear PIM1 localization (Fig. 11), since subcellular localization of PIM1 was reported to be associated with specific PIM1 function.

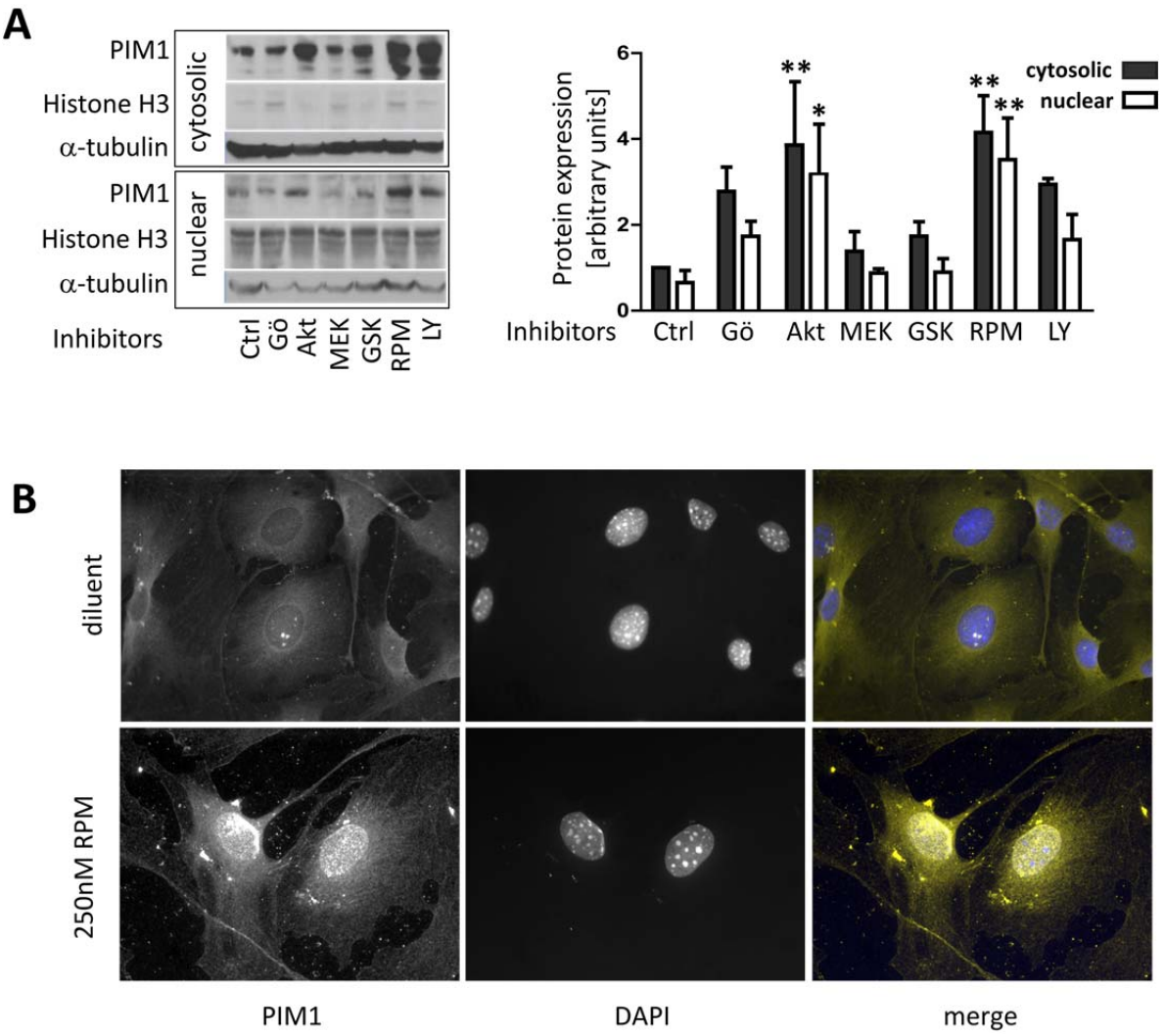

Figure 11. Akt and rapamycin inhibition increases PIM1 expression levels. (A) PIM1 expression levels of cytosolic and nuclear fractions from MAEC treated with inhibitors of different signaling cascades (left panel). Corresponding densitometric quantification of PIM1 expression levels. (right panel) **(B)** Immunofluorescence image of endogenous PIM1 after 3 hours of rapamycin treatment (lower panel) and control (upper panel). Endogenous PIM1 (left panel), nuclei (middle panel) and merge (right panel). In the merge picture the nuclei are displayed in blue and PIM1 kinase in yellow. (n=3). **P*<0.05, ***P*<0.01

PIM1 protein expression levels from cytosolic and nuclear fractions were quantified after 3 hours of treatment with the inhibitors. We found that mTOR and AKT inhibition significantly increased PIM1 expression both in cytosolic and nuclear fractions with no significant alterations in subcellular distribution (Fig. 11A). PIM1 was upregulated 3.9 fold after AKT inhibition and 4.2 fold after mTOR inhibition by rapamycin in the cytosolic fractions. It was upregulated 4.7 and 5.2 fold, respectively, in nuclear fractions. We observed an upregulation of PIM1 in the cytoplasm and the nucleus after 3 hours of rapamycin treatment, as visualized by immunofluorescence analysis (Fig. 11B).

Thus, rapamycin inhibited proliferation of endothelial cells lacking PIM1 more effectively. On the other hand, rapamycin increased PIM1 protein expression, both within the cytosol and nucleus. Based on these data, we formulated the hypothesis, that PIM1 may exert a function in the nucleus that counteracts or partially rescues decrease in proliferation in response to inhibition by mTOR.

To test this hypothesis, we constructed a vector-based *Pim1* expression system with PIM1 mutations that localize exclusively to the nucleus.

7.3 Generation of *Pim1* expression systems

7.3.1 Generation of a dsRED-Pim1 expression system

To re-express *Pim1* in MAEC, we generated a dsRED-*Pim1* expression vector. *Pim1* cDNA was cloned into a pdsRED C1 expression vector (Fig. 12A lower panel). The tag was N-terminally linked to *Pim1* cDNA (Fig. 12A upper panel). dsRED-*Pim1* was then transfected into *Pim1*$^{-/-}$ MAEC and the transfection efficiency was assessed by immunofluorescence microscopy and counted as 50-60% (data not shown). Fig. 12B shows a single aortic endothelial cell expressing dsRED-PIM1.

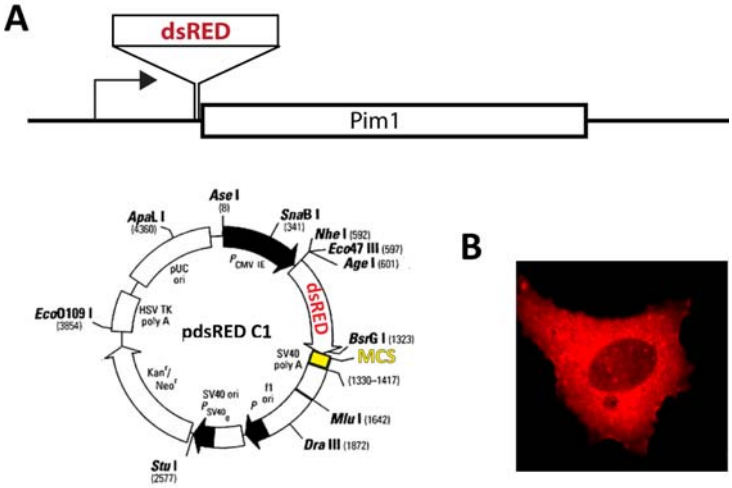

Figure 12. dsRED-*Pim1* expression system. (A) Schematic representation of the Pim1 cDNA (upper panel) inserted in a pdsRED C1 expression vector (lower left panel). (B) *Pim1*$^{-/-}$ MAEC expressing dsRED-*Pim1* (red). MCS: multiple cloning site (yellow).

7.3.2 Generation of a FLAG-Pim1 expression system

We generated a second expression system with a low molecular weight tag. To do so, *Pim1* cDNA was cloned into a pCMV-Tag 2A expression vector (Fig.13A lower panel).

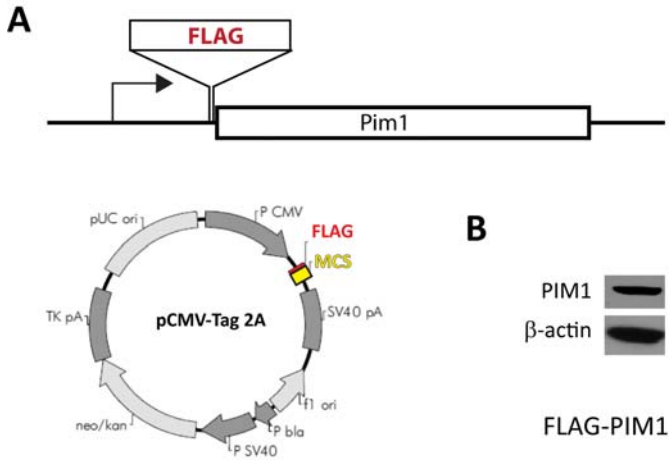

Figure 13. FLAG-*Pim1* expression system. (A) Schematic representation of the *Pim1* cDNA (upper panel) inserted in a pCMV-Tag 2A (lower left panel) expression vector. (B) Whole cell lysate of *Pim1*$^{-/-}$ MAEC expressing FLAG-*Pim1*. MCS: multiple cloning site.

As with the pdsRED-*Pim1* vector, the FLAG-tag was N-terminally linked to *Pim1* cDNA (Fig.13A upper panel). FLAG-*Pim1* was then re-expressed in *Pim1*$^{-/-}$ MAEC and protein expression levels assessed by Western blot (Fig.13B).

7.3.3 Generation of a FLAG-Pim1/dsRED-Pim1 carboxy-terminal truncations

PIM1 nuclear localization has been proposed to depend on half of its carboxy terminus (C-terminus) [89]. Our in silico analysis using the open access NucPred software (www.sbc.su.se/~maccallr/nucpred) revealed no nuclear localization signal (data not shown). mTOR has been shown to regulate cytoplasmic/nuclear shuttling of Nuclear factor of activated T-cells cytoplasmic 4 (NFATc4) by phosphorylation [90]. We therefore tested whether a similar mechanism could influence the increase of PIM1 nuclear localization. To identify critical phosphorylation sites, i.e., minimal critical C-terminal truncations responsible for PIM1 nuclear localization we generated dsRED-*Pim1* and FLAG-*Pim1* carboxy-terminal mutations with truncation at potential mTOR-phosphorylation sites. As shown in Fig. 14, *Pim1* cDNA was truncated at the first seven putative phosphorylation sites: Ser312, Ser308, Ser306, Ser276, Ser261, Ser260, Ser227 (Serine).

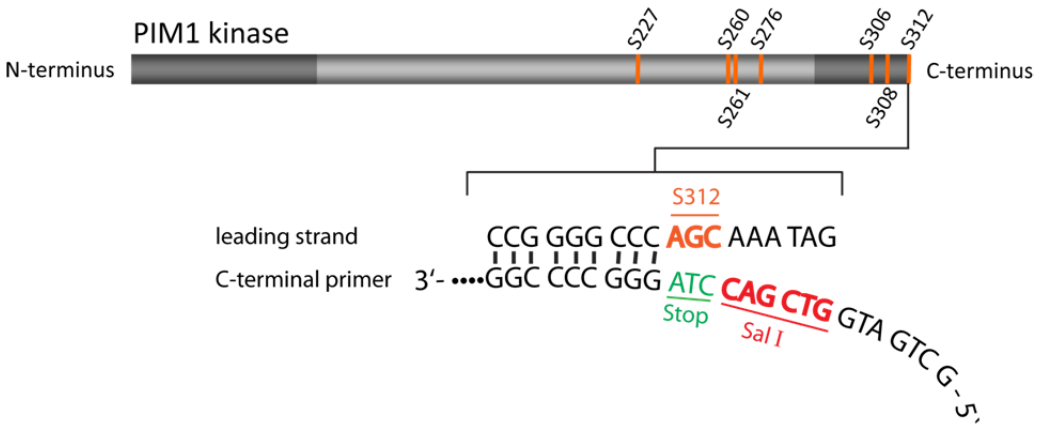

Figure 14. C-terminal truncation sites of PIM1 kinase. Schematical representation of PIM1 kinase with the serines of interest shown in orange (upper part). Scheme how the C-terminal primers bind to the leading strand (lower part). S: Serine (orange), Stop: Stop codon (green), Sal I: restriction site (red), N-terminus: Amino-terminus, C-terminus: carboxy-terminus.

Therefore, *Pim1* cDNA was amplified, with primers containing the appropriate restriction sites for insertion into pdsRED C1 or pCMV-Tag 2A expression vector at 5'- and 3'-ends. While the amino-terminal primer remained the same for each reaction, the carboxy-terminal primers were designed to bind beyond the appropriate serine followed by a stop codon each (Fig. 14).

7.4 Truncation of C-terminal residues of dsRED-*Pim1* beyond Serine 276 (*Pim1*$^{\Delta 276\text{-}313}$) results in an increased number of PIM1 nuclear positive cells.

Full length dsRED-*Pim1* (*Pim1*^{wt}) treated with or without rapamycin and dsRED-*Pim1* truncation mutants (*Pim1*$^{\Delta 227-313}$) were re-expressed in *Pim1*$^{-/-}$ MAEC. Cells positive for nuclear PIM1 protein were quantified by immunofluorescence microscopy (Fig.15).

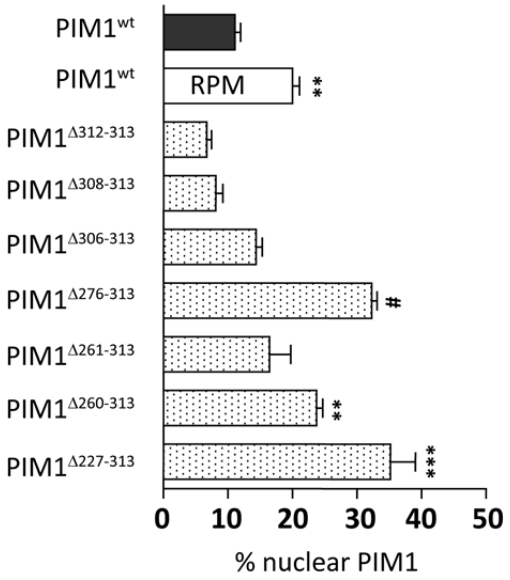

Figure 15. Percentage of nuclear PIM1 positive *Pim1*$^{-/-}$ cell cultures, transfected with dsRED-*Pim1* wildtype (black bar), dsRED-*Pim1* wildtype with RPM (open bar) and c-terminal truncation mutants *Pim1*$^{\Delta 313\text{-}227}$ (spotted bar). Data are represented as means ± s.e.m. (n=3). $^{**}P<0.05$, $^{***}P<0.005$, $^{\#}P<0.0001$.

Cell cultures of MAEC expressing PIM1^{wt}, treated for 3 hours with rapamycin, displayed a 1.88-fold increase in nuclear PIM1 compared to untreated cells. MAEC

transfected with *Pim1*$^{\Delta 312-313}$, *Pim1*$^{\Delta 308-313}$ and *Pim1*$^{\Delta 312-313}$ showed no significant increase in nuclear PIM1 positive cells. However, except for MAEC transfected with truncation mutant *Pim1*$^{\Delta 261-313}$, c-terminal truncations beyond Serine 276, displayed a significantly higher percentage of PIM1 nuclear positive cells: *Pim1*$^{\Delta 276-313}$ 2.9 fold, *Pim1*$^{\Delta 260-313}$ 2.2 fold and *Pim1*$^{\Delta 227-313}$ 3.2-fold compared to *Pim1*^{wt} transfected cells.

7.5 Truncation of C-terminal residues of FLAG-*Pim1* beyond Serine 276 (*Pim1*$^{\Delta 276-313}$) results in nuclear localization of the kinase and an increases MAEC proliferation.

The same experiment was also performed with the FLAG-*Pim1* constructs that were re-expressed in *Pim1*$^{-/-}$ cells (Fig.16A).

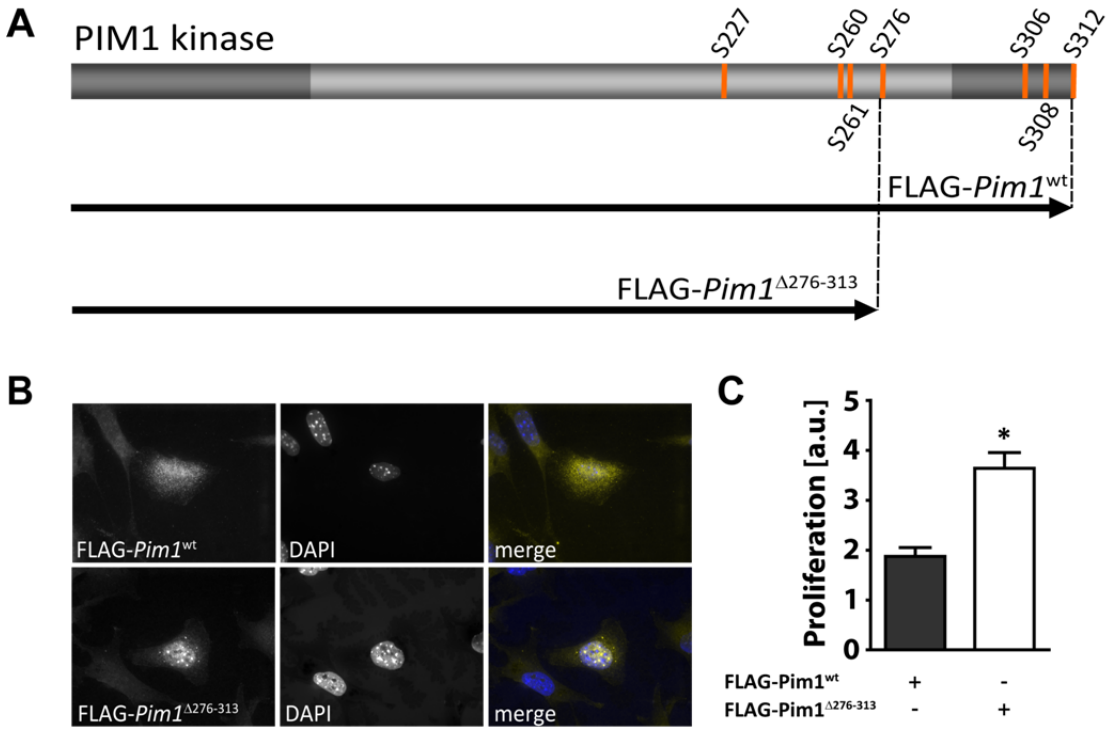

Figure 16. FLAG-*Pim1*$^{\Delta 276-313}$ localizes to the nucleus. (A) Scheme of the two truncations constructs, FLAG-*Pim1*^{wt} and FLAG-*Pim1*$^{\Delta 276-313}$ transfected into *Pim1*$^{-/-}$ MAEC. **(B)** MAEC transfected with FLAG-*Pim1*^{wt} (upper panel) and FLAG-*Pim1*$^{\Delta 276-313}$ (lower panel) cDNA. FLAG-*Pim1* (left panel), nuclei (middle panel) and merge (right panel). In the merge picture the nuclei are displayed in blue and PIM1 kinase in yellow. **(C)** Proliferation measurement of *Pim1*$^{-/-}$ MAEC re-expressing FLAG-*Pim1*^{wt} and FLAG-*Pim1*$^{\Delta 276-313}$. Data are represented as means ± s.e.m. (n=3). **P*<0.005.

Fluorescence microscopy using anti-FLAG antibodies revealed that only *Pim1* truncations beyond serine 276 resulted in nuclear translocations, whereas smaller truncations retained an even distribution of PIM1 in the cytosol (Fig.16B). In order to investigate whether phosphorylation of the sites around and at serine 276 is critical for nuclear localization, we generated Serine-phosphorylation and Serine-dephosphorylation mimicking mutants. This was performed by site directed mutagenesis of the serines 276, 261 and 306 into either an Alanine (Ala) or a Glutamate (Glu). Re-expression of these phosphorylation mimicking mutants in *Pim1*$^{-/-}$ cells revealed an inconsistent picture, which did not enable us to pinpoint one specific Serine residue to be responsible for nuclear translocation (data not shown). We therefore continued with the FLAG-*Pim1*$^{\Delta 276\text{-}313}$ truncation mutant that was consistently found in the nucleus to perform proliferation experiments. FLAG-*Pim1*^{wt} and FLAG-*Pim1*$^{\Delta 276\text{-}313}$ were overexpressed in *Pim1*$^{-/-}$ cells and cell proliferation was assessed (Fig.16C). Interestingly *Pim1*$^{-/-}$ MAEC expressing FLAG- *Pim1*$^{\Delta 276\text{-}313}$ displayed a 1.94 fold higher proliferation than cells expressing full length FLAG-*Pim1*.

8 RATIONALE AND AIMS OF THE 2ND PART OF THE THESIS

Elevated *Pim1* mRNA and protein levels correlate with the metastatic potential of tumors by facilitating migration and anti-adhesion [73-75]. Vice versa, inhibition of PIM1 kinase activity diminishes cancer cell migration and invasion in vitro [10, 75]. Endothelial cells play a pivotal role in these processes by contributing a barrier to the blood stream. PIM1 has been shown to be expressed in endothelial cells during in vivo angiogenesis and to be sensitive to VEGF in vitro [66]. In solid tumors, a prerequisite for cancer cell extravasation is alteration of endothelial cell barrier function, known to be associated with changes in expression of molecules important for endothelial cell adhesion [39, 91, 92]. However, so far no studies in endothelial cells exist, analyzing PIM1 function in endothelial barrier function. Here we investigated whether PIM1 regulates MAEC monolayer integrity.

Specifically my goals were:

- To functionally characterize adhesion properties of MAEC with deleted or inactivated PIM1 kinase.
- To determine the molecules which are differentially expressed in the adhesive phenotype of *Pim1*$^{-/-}$ MAEC.

9 RESULTS PART II :

Pim1 knockout imposes a superadhesive phenotype on endothelial cells

9.1 Pim1 kinase deletion and inhibition slows endothelial cell detachment by trypsinization and increases cell adhesion.

To investigate whether PIM1 influences endothelial cell adhesion characteristics we started with assessing resistance of electric current across endothelial monolayers (electric cell impedance sensing (ECIS)) and trypsin-mediated cell detachment after PIM1 kinase inhibitor treatment. Confluent wildtype MAECs were treated with the imidazo[1,2-b]pyridazine compound K00486, a kinase inhibitor reported to inhibit human PIM1 kinase activity in vitro [93]. The resistance of the cell monolayer was recorded for 24 hours at a frequency of 4kHz using ECIS (Fig. 18A). Compared to control, we observed a significant increase of 80 ± 5 ohm of total resistance at 4kHz in cells treated with K00486, indicating the formation of a tighter cell monolayer.
In parallel, MAECs were trypsinized 24 hours after seeding, and the detachment process was followed in a time course (Fig. 18B): A significant delay in the detachment of inhibitor-treated versus untreated cells was observed as early as after 2 min (9±0.002% vs. 23±0.01% of detached cells in the supernatant) of trypsinization. The difference in detachment remained significant also for later time points (n=3, P<0.0001). Even though the PIM1 inhibitor K00486 has been suggested to inhibit only PIM1 kinase [93] we could not exclude unspecific inhibition by this compound.
To further substantiate our findings of increased endothelial cell adhesion after PIM1 inhibition, we isolated MAECs from mice deficient for PIM1 [64] and corresponding control mice. *Pim1* mRNA and protein expression in the isolated cells was assessed using quantitative real-time PCR (qRT-PCR) (Fig. 18C) and Western blotting (Fig. 18D) confirming the knockout of *Pim1*. Trypsin treatment of these cells for 0, 1, 2, 3, 4 and 5 minutes displayed a marked resistance to trypsinization and detachment of endothelial cells lacking PIM1. After 3 minutes, only 5±1% $Pim1^{-/-}$ cells were detached compared to 36±3% of wildtype cells (n=3, P<0.001). Similarly, after 5

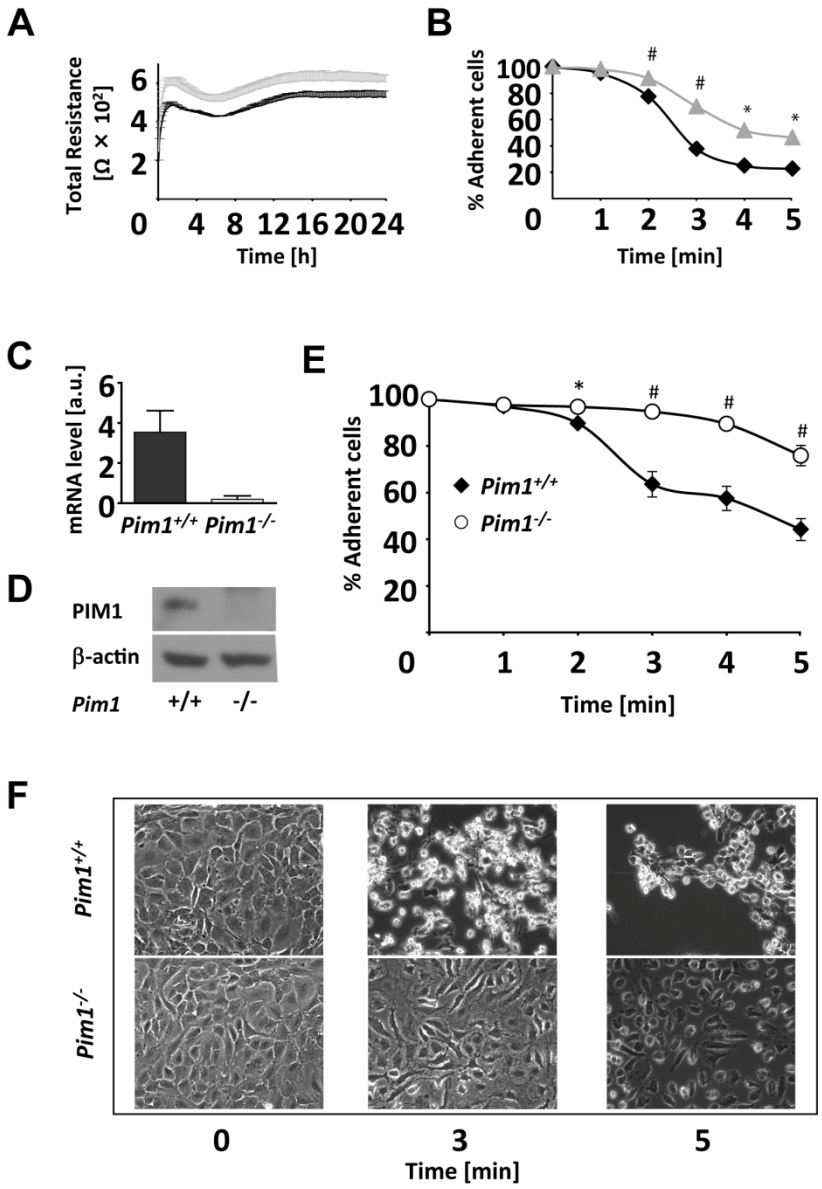

Figure 18. Detachment of wildtype and *Pim1*$^{-/-}$ endothelial cells after trypsinization. (A) Time course of total resistance at 4 kHz of endothelial control and cells treated with K00486 over a period of 24 hours using ECIS. **(B)** Time course displaying number of cells detached represented as percentage of total adherent cells; control vs. cells treated with K00486. **(C)** Steady state mRNA expression levels of wildtype and *Pim1*$^{-/-}$ cells. **(D)** Corresponding Western blot of wildtype and *Pim1*$^{-/-}$ cells. **(E)** Time course displaying number of cells detached represented as percentage of total adherent cells; wildtype vs. *Pim1*$^{-/-}$cells. **(F)** Representative micrographs of wildtype and *Pim1*$^{-/-}$ cells before and after 3 and 5 minutes of trypsin treatment. β-actin was used as loading control. Black symbols indicate wildtype, grey wildtype with K00486 and open *Pim1*$^{-/-}$ cells. Data are represented as means ± s.e.m. (n=3). **P*<0.05, $^{\#}$*P*<0.0001.

minutes, *Pim1*$^{-/-}$ MAECs number in the supernatant was significantly lower (n=3, *P*<0.001) (Fig. 18E), which is also visible in corresponding micrographs (Fig. 18F).

9.2 *Pim1*$^{-/-}$ decreases cell migration in a wound healing assay.

The differences in cell adhesion properties suggested that the migratory response of *Pim1*$^{-/-}$ cells might be also affected. We therefore investigated cell motility (Fig. 19).

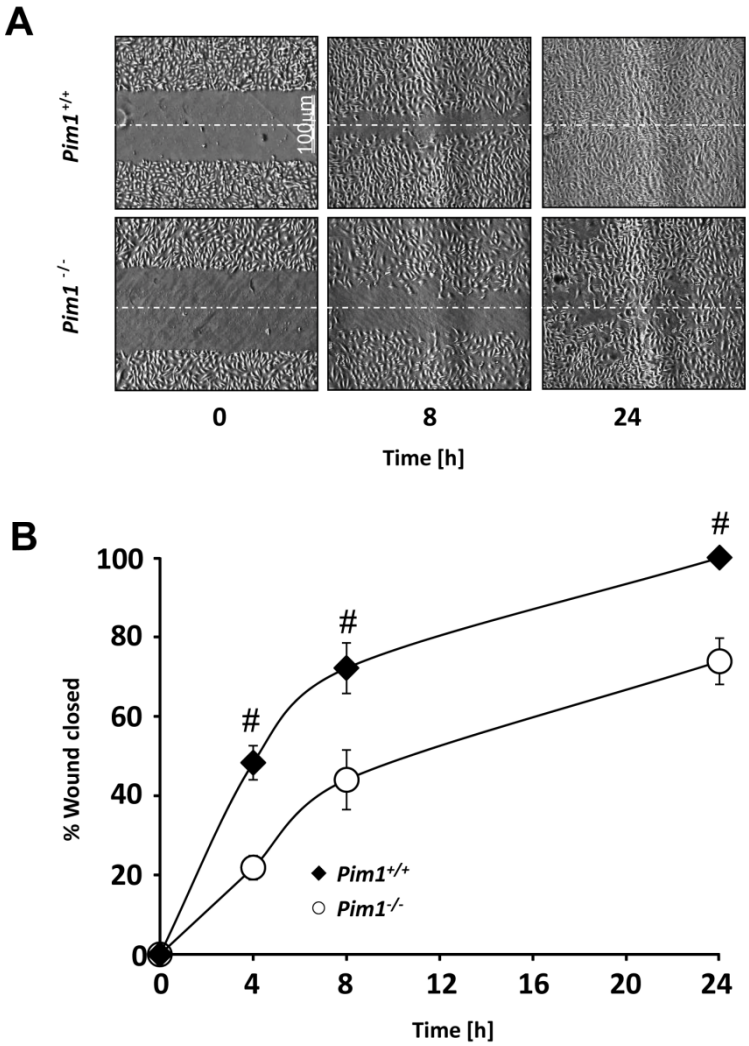

Figure 19. Wound healing assay comparing wildtype and *Pim1*$^{-/-}$ MAEC. (A) Micrographs from wildtype (upper panel) and Pim1-/- (lower panel) cells 0, 8 and 24 hours after wounding. (B) Corresponding time course displaying the percentage of recolonized wound after 0, 4, 8 and 24 hours of cell migration. Black symbols indicate wildtype and open *Pim1*$^{-/-}$ cells. Data are represented as means ± s.e.m. (n=5). #P<0.0001

Confluent wildtype and *Pim1*$^{-/-}$ endothelial monolayers were scratched and cell reinvasion into the wound was recorded over 24 hours. Quantification of the light micrographic pictures (Fig. 19A) revealed a 28.1±1.3% lower migration rate for *Pim1*$^{-/-}$ cells (Fig. 19B).

9.3 *Pim1*$^{-/-}$ MAECs form tighter cell-substratum and cell-cell contacts.

Adhesion properties of wildtype and *Pim1*$^{-/-}$ cells were further analyzed using ECIS. Cells were seeded at confluence, and total resistance of cell layers was measured during 24 hours at a frequency of 4kHz.

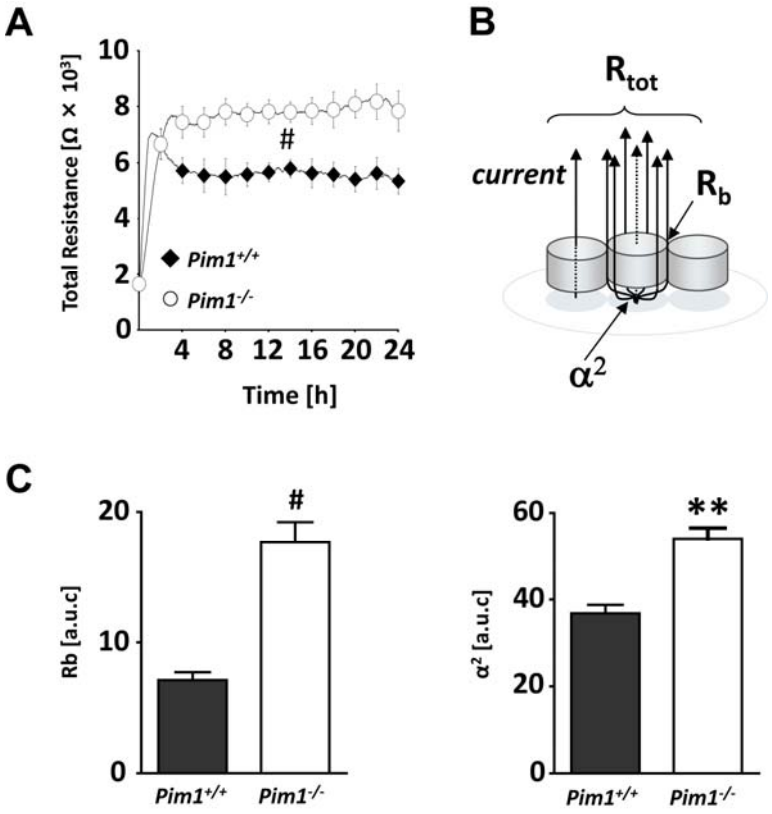

Figure 20. Real-time monitoring of adhesion process and monolayer formation in wildtype and Pim1-/- MAECs. (A) Time course of total resistance at 4 kHz of endothelial wildtype and Pim1-/- endothelial cells over a period of 24 hours using ECIS. (B) Schematic view of an ECIS plate coated with cells. R_{tot}: total resistance (cell occupancy); R_b: resistance between the cells; α^2: cleft impedance parameter; (C) α^2 value and R_b value measurement of the confluent cell layers from 8 to 24 hours. Wildtype (filled symbols) and *Pim1*$^{-/-}$ (open symbols). Bars represent the area under the curve (a.u.c.) from 8 to 24 hours as means ± s.e.m. (n=3). $^{**}P<0.001$, $^{\#}P<0.0001$.

After 8 hours the cells formed a confluent monolayer at the resistance value of 5600 ± 200 ohm for wildtype and 7800 ± 200 ohm for *Pim1*$^{-/-}$ cells (n=3, *P*<0.0001, Fig. 19A).

The ECIS model allows to differentiate between tightness of cell-cell contacts (R_b) and the strength of the cell-substratum adhesion (α^2) (Fig. 20B) [94, 95]. Area under the curve (a.u.c.) analysis for these parameters from 8 to 24 hours indicated a significant 2.3-fold of R_b (n=3, *P*<0.0001) and a 1.5-fold increase (n=3, *P*<0.0003) of α^2 respectively, in *Pim1*$^{-/-}$ cells (n=5, *P*<0.001) (Fig. 20C). Thus, *Pim1* deletion in endothelial cells markedly and significantly strengthens cell-cell and cell-substratum adhesion as judged from the R_b and α^2 value.

9.4 Expression of PIM1 leads to a decrease in total resistance of endothelial *Pim1*$^{-/-}$ cells.

To assess whether the hyper-adhesive properties of *Pim1*$^{-/-}$ cells might be indeed a consequence of loss of PIM1, we aimed to restore the phenotype by reintroduction of FLAG-*Pim1* cDNA into knockout cells. The amount of re-expressed FLAG-*Pim1* was determined by qRT-PCR and adjusted to similar levels of endogenous *Pim1* mRNA (Fig. 21A).

We measured the total resistance of *Pim1*$^{-/-}$ cells expressing FLAG-*Pim1* cDNA, wildtype and *Pim1*$^{-/-}$ cells transfected with control plasmid during 24 hours. Attachment and plateau establishment were not significantly changed in *Pim1*$^{-/-}$ and *Pim1*$^{-/-}$ cells after FLAG-*Pim1* cDNA expression. However, after 16 hours of measurement the electrical resistance of cells expressing FLAG-*Pim1* significantly decreased compared to *Pim1*$^{-/-}$ cells. After 24 hours the rescue effect in *Pim1*$^{-/-}$ cells expressing FLAG-*Pim1* reached a maximum of approximately 40% reduction to wildtype resistance values (Fig. 21B).

Area under the curve analysis for the strength of cell-substratum adhesion and tightness of cell-cell contacts from 8 to 24 hours was calculated for wildtype, *Pim1*$^{-/-}$ and *Pim1*$^{-/-}$ cells expressing FLAG-*Pim1*. Reintroduction of FLAG-*Pim1* into wildtype or *Pim1*$^{-/-}$ cells did not affect α^2-value (Fig. 21C). However, the difference in the area under the curve (a.u.c.) for R_b between wildtype and *Pim1*$^{-/-}$ cells was reduced by

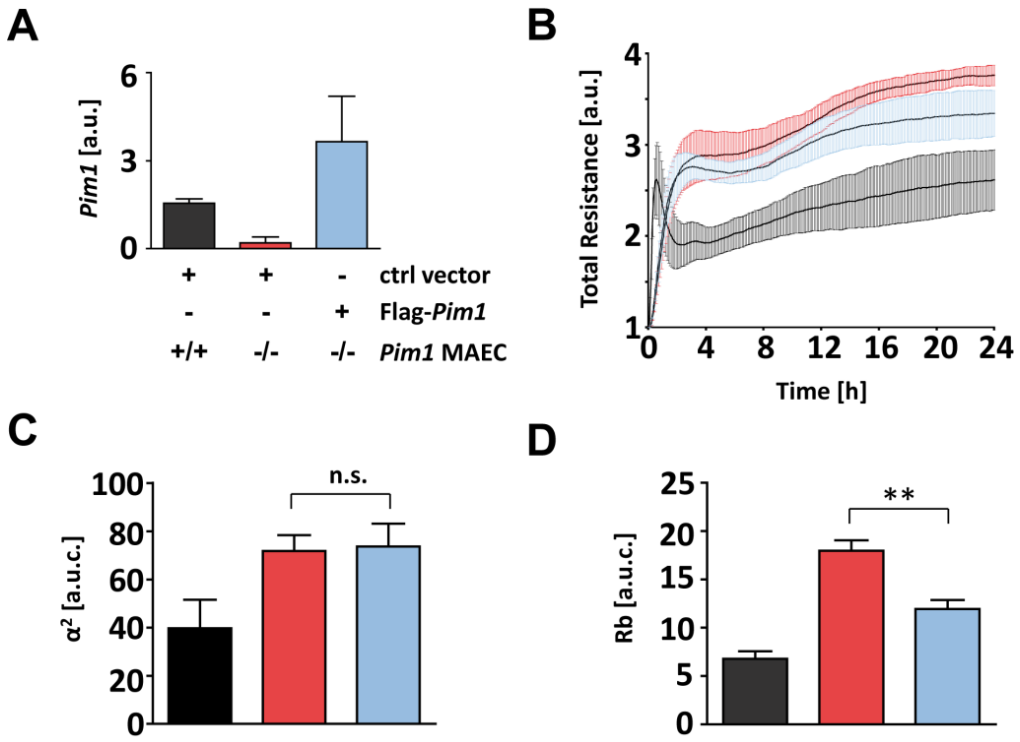

Figure 21. ECIS analysis of Pim1-/- cells after FLAG-Pim1 cDNA re-expression. (A) qRT-PCR of endogenous Pim1 from wildtype and Pim1-/- cells and Pim1-/- cells transiently transfected with FLAG-Pim1 cDNA, quantified with primers amplifying the FLAG sequence. **(B)** Determination of total resistance at 4 kHz during 24 hours from wildtype, *Pim1*$^{-/-}$ and FLAG-*Pim1* expressing *Pim1*$^{-/-}$ cells. **(C)** Area under the curve analysis of α^2 value from 8 to 24 hours of wildtype, *Pim1*$^{-/-}$ cells and *Pim1*$^{-/-}$ cells transfected with FLAG-*Pim1* cDNA. **(D)** Area under the curve analysis of R_b from 8 to 24 hours of wildtype, *Pim1*$^{-/-}$ cells and *Pim1*$^{-/-}$ cells transfected with FLAG-*Pim1* cDNA (left panel) with the corresponding resistance value curves (right panel). Resistance values were normalized to value 1 at time point 0 hours. Arbitrary units (a.u.) wildtype (black), *Pim1*$^{-/-}$ (red), *Pim1*$^{-/-}$ transfected with FLAG-*Pim1* (blue). Data are represented as means ± s.e.m. (n=3). ***P*<0.001.

54% (n=3, *P*<0.001) when re-expressing FLAG-*Pim1* in *Pim1*$^{-/-}$ cells (Fig. 21D) Thus, reintroduction of Pim1 cDNA into *Pim1*$^{-/-}$ MAEC restores R_b values to more than half of that of R_b wildtype levels.

9.5 Endothelial cell-cell junctions and focal adhesion structures are more pronounced in *Pim1* knockout cells.

β-catenin is a protein of the adherens junction complex and vinculin is an ubiquitary expressed protein involved in focal adhesion and also cell-cell contact formation [96, 97].

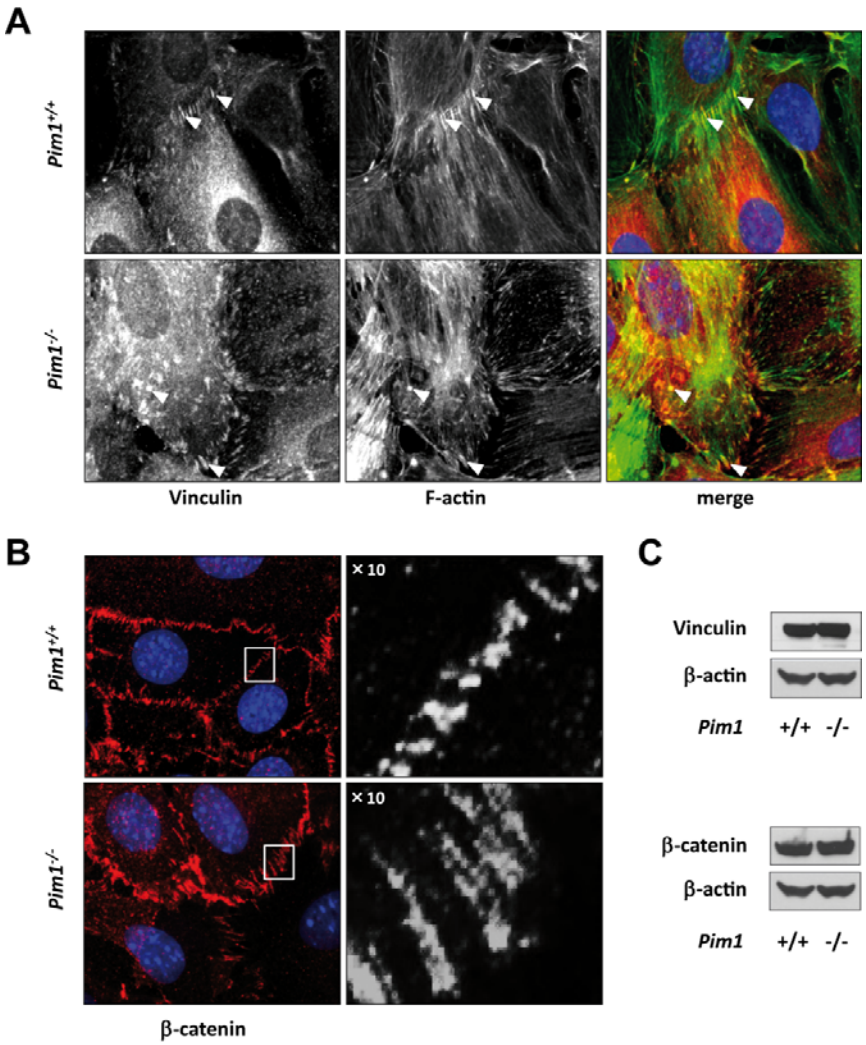

Figure 22. Vinculin and β-catenin protein expression analysis. (A) Vinculin immunofluorescence images of MAEC, wildtype (upper left panel) vs. *Pim1*$^{-/-}$ (lower left panel) and F-actin staining of the corresponding area (middle panel). Merge of vinculin (red) and F-actin (green) images (left panel). **(B)** β-catenin (red) immunofluorescence images of wildtype (upper panel) and *Pim1*$^{-/-}$ (lower panel) MAEC. On the right a corresponding 10 times magnification of the area is indicated by a white rectangle. **(C)** Western blot of vinculin (upper panel) and β-catenin (lower panel) from wildtype and *Pim1*$^{-/-}$ whole cell lysates. The nuclei are shown in blue. White arrows indicate the overlapping regions (yellow) (Total magnification ×100).

To validate the increased resistance in cell adherens junctions and focal adhesions observed by ECIS, we assessed the protein expression levels of β-catenin and vinculin by immunofluorescence imaging and Western blot (Fig. 22). Fluorescence imaging disclosed a much more prominent vinculin patterning in *Pim1*$^{-/-}$ cells: The knockout cells formed more vinculin clusters around the cell (white arrows) (Fig. 22A left panel). Additionally also F-actin, which is bound by vinculin, was stained (Fig. 22A middle panel). The overlay of vinculin and actin stainings visualizes the difference in the amount of focal adhesion clusters (Fig. 22A right panel).

To investigate whether we also may find distinct changes in adherens junctions we stained for β-catenin in wildtype and knockout cells (Fig. 22B left panel). Indeed the β-catenin clusters were expanded in *Pim1*$^{-/-}$ cells, which is also visualized in a 10-times magnification in Fig. 22B right panel. Nevertheless, we found no changes in overall protein expression of β-catenin and vinculin when comparing wildtype and *Pim1*$^{-/-}$ cells (Fig.22C).

9.6 Gene expression analysis reveals importance of PIM1 in cell adhesion and cytoskeleton remodeling.

To obtain a more global view of the capacity of PIM1 to regulate cell adhesion we compared mRNA expression of wildtype and *Pim1*$^{-/-}$ cells using a two color Agilent DNA microarray.

Analysis of the gene expression data revealed 1598 significantly regulated genes (P<0.01) from which 61% were up- and 39% downregulated. The most regulated genes include *Foxg1* with a ratio of 200-fold upregulation and *Eif2s3* with a 70-fold downregulation (Table 3).

Gene Symbol	Acc. No.	Ratio	Gene Name	*P*-Value
Genes upregulated by *Pim-1*knockout				
Foxg1	NM_008241	214.9	*forkhead box G1*	0.00002
Fhl1	NM_010211	199	*four and a half LIM domains 1*	0.00010
Col6a3	NM_009935	77.26	*collagen, type VI, alpha 3*	0.00067
Sfrp2	NM_009144	35.64	*secreted frizzled-related protein 2*	0.00114
Ccdc68	NM_201362	31.66	*coiled-coil domain containing 68*	0.00158
Xlr4b	NM_021365	31.4	*X-linked lymphocyte-regulated 4B*	0.00115
Lhx9	NM_010714	30.16	*LIM homeobox protein 9*	0.00028
Gsta1	NM_008181	21.62	*glutathione S-transferase*	0.00142
Col11a1	NM_007729	21.11	*collagen, type XI, alpha 1*	0.00013
Serpine2	NM_009255	20.13	*serine (or cysteine) peptidase inhibitor, clade E, member 2*	0.00003
Genes downregulated by *Pim-1*knockout				
Eif2s3y	NM_012011	71.32	*eukaryotic translation initiation factor 2, subunit 3, structural gene Y-linked*	0.00085
Gdf10	NM_145741	40.39	*growth differentiation factor 10*	0.00404
Thumpd1	NM_145585	29.63	*THUMP domain containing 1*	0.00075
Svep1	NM_022814	25.24	*sushi, von Willebrand factor type A, EGF and pentraxin domain containing 1*	0.00048
Ddx3y	NM_012008	24.28	*DEAD (Asp-Glu-Ala-Asp) box polypeptide 3, Y-linked*	0.00260
Serpina3g	NM_009251	22.76	*serine (or cysteine) peptidase inhibitor, clade A, member 3G*	0.00493
Tbx1	NM_011532	14.37	*T-box 1*	0.00017
Svep1	NM_022814	13.87	*sushi, von Willebrand factor type A, EGF and pentraxin domain containing 1*	0.00035
Cfh	NM_009888	12.60	*complement component factor h*	0.05249
Frzb	NM_011356	12.55	*frizzled-related protein*	0.00309

Table 3. Expression of differently expressed genes in *Pim1*$^{-/-}$ MAECs as identified by microarray analysis.

Single genes were summarized by their biological function using MetaCore™ analysis. Intriguingly, four out of ten most significantly regulated biological processes were computed as cell adhesion, migration and cytoskeleton remodeling (Table 4). This assignment is in line with our cell biological assessment.

Biological Process		Description	*P*-Value
Cytoskeleton remodeling :		TGF and WNT mediated cytoskeleton remodeling	2.03E-06
Signal transduction	:	Inhibition of Erk	3.03E-06
Cell adhesion	:	Histamine H1 receptor signaling in the interruption of cell barrier integrity	3.03E-06
Cell adhesion	:	Integrin-mediated cell adhesion and migration	5.34E-06
Immune response	:	CCR3 signaling in eosinophils	7.69E-06
Chemotaxis	:	Inhibitory action of lipoxins on IL-8- and Leukotriene B4-induced neutrophil migration	9.01E-06
Cytoskeleton remodeling :		Role of PKA in cytoskeleton reorganisation	1.09E-05
Development	:	Role of HDAC and calcium/calmodulin-dependent kinase (CaMK) in control of skeletal myogenesis	1.47E-05
Muscle contraction	:	GPCRs in the regulation of smooth muscle tone	1.61E-05
Migration	:	Inhibitory action of Lipoxins on neutrophils	2.31E-05

Table 4. Involvement of differently regulated genes in biological processes comparing *Pim1*$^{-/-}$ versus wildtype cells as analysed by GeneGo software (top down by *P*-value).

A specific gene set involved in cell adhesion was selected for further validation (Table 5).

Gene Symbol	Acc. No.	Ratio	Gene Name	*P*-Value
Genes upregulated by *Pim-1*knockout				
Col6a3	NM_009935	77.3	*procollagen, type VI, alpha 3*	0.0067
Col11a1	NM_007729	21.1	*procollagen, type XI, alpha 1*	0.0001
Itgb4	NM_001005608	14.1	*integrin beta 4*	0.0037
Cdh13	NM_019707	11.4	*cadherine 13 / T-cadherine*	0.0001
Icam1†	BC008626	5.9	*intercellular adhesion molecule 1*	0.0181
Itga7	NM_008398	3.8	*integrin alpha 7*	0.0001
Itga3	NM_013565	3	*integrin alpha 3*	0.0044
Jam2	NM_023844	2.609	*junction adhesion molecule 2*	0.0020
Genes downregulated by *Pim-1* knockout				
Svep1	NM_022814	25.64	*sushi, von Willebrand factor type A, EGF and pentraxin domain containing 1*	0.0005
Itga11	NM_176922	5.5	*integrin alpha 11*	0.0007
Adam23	NM_011780	4.9	*a disintegrin and metallopeptidase domain 23*	0.0020
Vcam1	NM_011693	3.1	*vascular cell adhesion molecule 1*	0.0009

Table 5. Genes involved in cell adhesion up- or downregulated in *Pim1*$^{-/-}$ cells. A cluster of genes which were found to be significantly regulated in the gene expression analysis was selected for further validation by qRT-PCR. (top down by ratio; *P*<0.05; †>0.05).

7 out of these 12 genes could be validated using qRT-PCR: the integrin family member *integrin alpha 7 (Itga7)*, the *junctional adhesion molecule 2 (Jam2)*, *T-cadherin* also known as *cadherin 13 (Cdh13)*, *a disintegrin and metalloproteinase domain-containing protein 23 (Adam23)*, the extracellular matrix proteins *collagen type VI, alpha 3 (Col6a3)*, *collagen type XI, alpha 1 (Col11a1)* and *sushi, von Willebrand factor type A, epidermal growth factor and pentraxin domain containing 1 (Svep1)* which belongs to a new group of membrane proteins involved in cell adhesion [98]. The most significantly regulated genes also displaying the highest mRNA expression levels in *Pim1*$^{-/-}$ cells were identified as *Col6a3* (fold induction = 51.6; *P*<0.0001), and *Cdh13* (fold induction = 81.9; *P*<0.0002) (Fig. 23A), both upregulated in *Pim1*$^{-/-}$ cells.

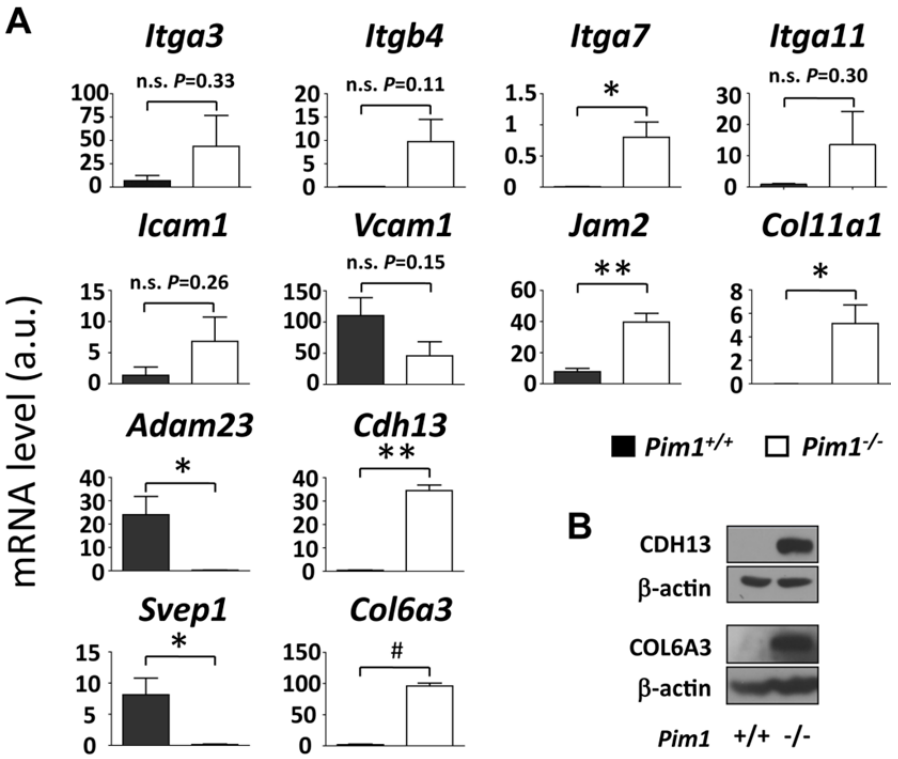

Figure 23. Validation of the adhesion cluster using qRT-PCR. (A) mRNA from wildtype and *Pim1*$^{-/-}$ MAECs was isolated after 24 hours and steady state expression levels of indicated genes were validated by qRT-PCR. **(B)** Western blot of CDH13 and COL6A3 from wildtype and *Pim1*$^{-/-}$ whole cell lysates. Data are represented as means ± s.e.m. (n=3). **P*<0.05, ***P*<0.001, $^{\#}$*P*<0.0001.

Figure 23B shows protein expression levels of CDH13 and COL6A3, proteins involved in cell-cell and cell substratum adhesion, respectively.

9.7 Pim1$^{-/-}$-deposited matrix induces adhesion characteristics of Pim1$^{-/-}$ cells in wildtype cells

Extracellular matrix deposition and composition is of fundamental importance in cell adhesion and migration [99]. We found significantly different gene expression of

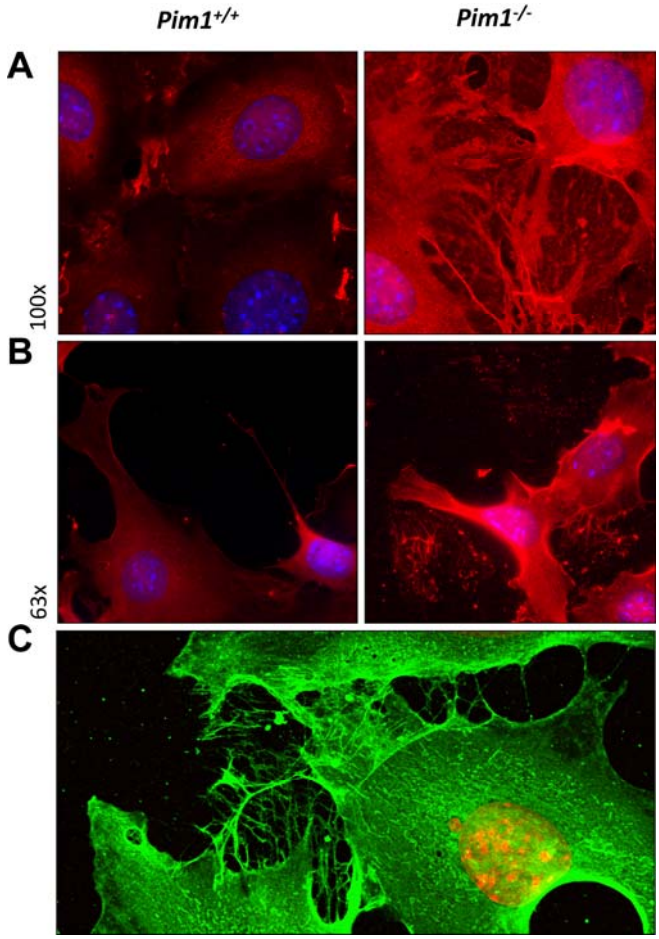

Figure 24. *Pim1*$^{-/-}$ but not wildtype MAEC display deposits of COL6A3-positive fibre-like structures outside cells. (A) Representative micrographs of COL6A3 (red) and nuclear (blue) immunestaining in confluent wildtype (left) and *Pim1*$^{-/-}$ (right) MAEC (n=3, magnification 100x). **(B)** Representative micrographs of COL6A3 (red) and nuclear (blue) immunestaining in subconfluent wildtype (left) and *Pim1*$^{-/-}$ (right) MAEC (n=3, magnification 63x). **(C)** Confocal image of a COL6A3 (green) immunestaining from *Pim1*$^{-/-}$ MAEC. Nuclei are shown in red. (magnification 100x).

matrix components and cell-matrix receptors, such as collagens and integrins. COL6A3 as the most strongly and significantly expressed matrix component was further examined by immunostaining. We found that confluent *Pim1*$^{-/-}$ but not wildtype MAEC expressed COL6A3 positive bundles inside the cells, extending in network-like structures on top of endothelial cells (Fig 24A, right micrograph). Furthermore, *Pim1*$^{-/-}$ but not wildtype MAEC deposited fibre-like structures containing COL6A3 between cells accumulating on the cell-free culture plate surface (Fig24B, right micrograph). Figure 24C shows a magnification of a COL6a3 immunostaining from *Pim1*$^{-/-}$ cells.

We therefore aimed at determining whether the adhesion properties of *Pim1*$^{-/-}$ cells also depend on this specific ECM deposition. Wildtype cells were cultivated on ECM deposited by wildtype or *Pim1*$^{-/-}$ cells (Fig. 25A).

Trypsin treatment of these confluent cells for 0, 1, 2 and 3 minutes displayed a marked delay of the detachment of wildtype endothelial cells cultured on matrix deposited by *Pim1*$^{-/-}$ cells (Fig. 25A). Wildtype cells remained attached to the *Pim1*$^{-/-}$ matrix to 84±1% in contrast to 52±8% on the wildtype matrix after 1 minute of trypsin treatment and three PBS washing steps (n=3, $P<0.003$). After three minutes and three PBS washing steps 63.2±13% of wildtype cells remained attached to the *Pim1*$^{-/-}$ matrix whereas only 16.8±12% of wildtype cells remained attached to the wildtype matrix (n=3, $P<0.02$).

To compare the degree to which *Pim1*$^{-/-}$ deposited matrix was able to induce adhesion characteristics of *Pim1*$^{-/-}$ cells in wildtype cells, we performed trypsinization experiments with confluent wildtype and *Pim1*$^{-/-}$ cells which were washed three times after three minutes of trypsin treatment. Again, supernatant was collected and cells counted. The washing steps decreased the number of wildtype MAEC remaining attached to the culture dish (21.7±1.8%), whereas *Pim1*$^{-/-}$ cells still resisted trypsinization (77.5±0.9%, n=5, $P<0.0003$) (Fig. 25B). The percentage of *Pim1*$^{-/-}$ cells remaining attached to the substratum was similar and statistically not different compared to the percentage of wildtype cells remaining attached to the *Pim1*$^{-/-}$ deposited matrix after three minutes of trypsin treatment ($P=0.47>0.05$, n=3) (Fig. 25B). Finally, we investigated, whether *Pim1*$^{-/-}$ cell-deposited matrix was sufficient to induce structural changes in adherens junctions of wildtype MAEC as observed in *Pim1*$^{-/-}$ cells (see Figure 22B). Indeed, when cultivating wildtype MAEC on *Pim1*$^{-/-}$

cell-deposited matrix and staining confluent cultures, we observed enhanced β-catenin containing structures at cell-cell borders (Figure 25C).

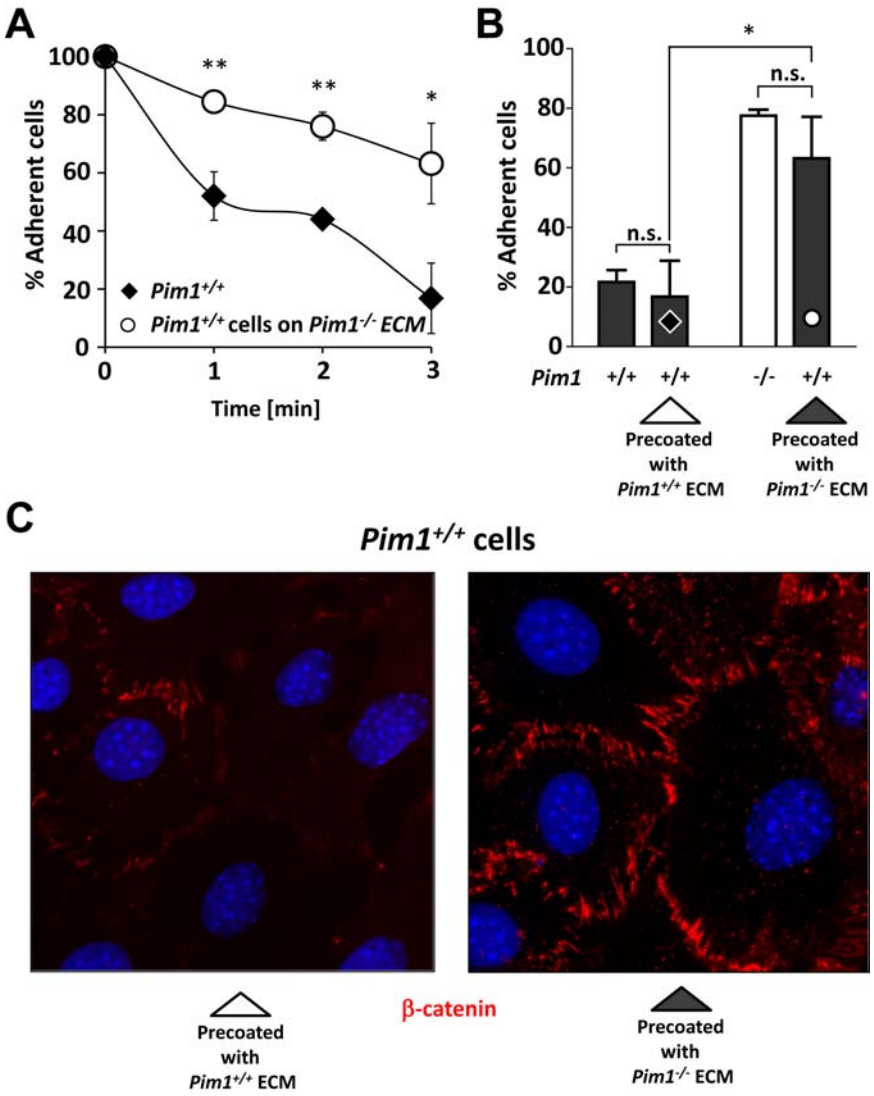

Figure 25. Detachment of wildtype cells grown on wildtype or *Pim1*$^{-/-}$ ECM compared to wildtype and *Pim1*$^{-/-}$ cells after trypsinization. (A) Time course represented as a percentage of adherent wildtype cells after 0, 1, 2 and 3 minutes of trypsin treatment, grown either on wildtype or *Pim1*$^{-/-}$ ECM. Wildtype cells grown on wildtype ECM are shown as black symbols and wildtype cells grown on *Pim1*$^{-/-}$ ECM as open symbols. **(B)** Corresponding graph after 3 minutes of trypsinization compared to wildtype and *Pim1*$^{-/-}$ cells grown on their intrinsic ECM. Wildtype cells are shown as black, knockout cells as white bars, wildtype cells on wildtype ECM as black bars with a black diamond and wildtype cells on knockout ECM as black bars with an open circle. **(C)** Immunofluorescent staining of β-catenin (red) and nuclei (DAPI, blue) of wildtype MAEC cultured on matrices deposited by wildtype MAEC (micrograph on the left) and by *Pim1*$^{-/-}$ MAEC (micrograph on the right; magnification 63x, n=3).Data are represented as means ± s.e.m. (n=3). **P*<0.05, ***P*<0.001, $^{\#}$*P*<0.0001.

Thus, ECM deposited by *Pim1*$^{-/-}$ cells is sufficient to mediate a hyperadhesive phenotype similar to that of *Pim1*$^{-/-}$ cells with respect to cell detachment and adherens junction strengthening.

10 DISCUSSION

In healthy conditions PIM1 kinase expression is low and no major phenotypes have been found in *Pim1*$^{-/-}$ animals so far [64]. However animals deficient for all three PIM kinases show reduced body size at birth and in vitro response of hematopoietic cell populations to growth factors was impaired [1]. PIM1 overexpression has been implicated in different types of cancer where it enhances cell proliferation and metastasis [75, 100]. In line with this, inhibition of PIM1 kinase activity diminishes cancer cell migration and invasion [10, 75]. Tumor progression and tumor cell extravasation not only depend on cancer cells. Angiogenesis and blood vessel permeability, i.e. endothelial monolayer integrity, are also critical determinants for cancer progression [9]. However, little is known about primary endothelial cell cultures and the impact of PIM1 kinase on endothelial barrier integrity.

Vessel growth is stimulated by proangiogenic factors and depends on cell proliferation and migration. Cell proliferation needs activation of specific signalling pathways involved in cell cycle progression. Rapamycin is a potent anti-proliferative drug, inhibiting the mTOR-pathway with different applications in clinical medicine [101]. Also in endothelial cells, rapamycin reduces proliferation and thereby angiogenesis [86, 102]. In T-lymphocytes, complete arrest of cell expansion by rapamycin is only observed in cells lacking PIM kinases [83]. Cell migration implies assembly and disassembly of cell to cell and cell to matrix adhesion sites and rearrangements of the actin cytoskeleton and the ECM. PIM1 silencing by RNAi diminished endothelial migration in response to VEGF [66], but so far no data on PIM1-dependent rearrangement of cell-cell and cell-matrix adhesion is available. Therefore, we investigated PIM1's involvement in endothelial cell proliferation with respect to rapamycin treatment and endothelial barrier integrity in wildtype and *Pim1*$^{-/-}$ cells.

We show, that proliferating *Pim1*$^{-/-}$ cells have an increased sensitivity to rapamycin. Furthermore, inhibition of the mTOR signaling pathway increased PIM1 cytosolic and nuclear protein levels. By overexpression of c-terminal truncated *Pim1* mutants we found a region to be critical for intracellular localization of the kinase. Finally, overexpression of this minimal c-terminal truncation of *Pim1* (FLAG-*Pim1*$^{\Delta 276\text{-}313}$), which localizes to the nucleus, increased proliferation of *Pim1*$^{-/-}$ cells significantly.

Pim1 deletion and kinase inhibition attenuated endothelial cell detachment by trypsinization and increased total electrical resistance across the endothelial monolayer. Reintroduction of *Pim1*-cDNA into *Pim1*$^{-/-}$ cells partially but significantly restored electrical resistance to wildtype levels. Furthermore, *Pim1* depleted endothelial cells had markedly reduced cell motility as shown in wound healing assays. On the level of gene regulation, this phenotype caused expressional changes of a subset of cell-cell attachment proteins and cell adhesion molecules. Additionally, protein abundance of β-catenin and vinculin, at the adherens and tight junctions, was markedly increased. Intriguingly, ECM deposited by *Pim1*$^{-/-}$ cells alone was sufficient to induce *Pim1*$^{-/-}$ adhesion characteristics in wildtype cells.

10.1 *Pim1* knockout increases sensitivity of MAEC proliferation to rapamycin.

During the past years rapamycin and rapalogues have emerged as anticancer drugs for several specific cancers. Nevertheless, these reagents have turned out to be less efficacious in tumor treatment than expected [103]. Our first observation in MAEC was a marked increase of PIM1 protein levels after rapamycin treatment (Fig.11). As PIM1 has been shown to inactivate cell cycle inhibitors such as p27^{Kip1} [77] or p21$^{Cip1/Waf1}$ [78], we asked whether this could be a refractory mechanism to mTOR inhibition. Indeed, compared to wildtype cells, *Pim1*$^{-/-}$ MAEC proliferation showed a significantly increased sensitivity to rapamycin (Fig.10A). PIM kinases also mediate survival signaling by interaction with members of the BCL2 protein family [104] and partially through direct phosphorylation of the pro-apoptotic protein BAD [65, 81]. To differentiate if decrease in *Pim1*$^{-/-}$ cell proliferation was partially due to cell death, we analyzed cell survival by FACS. However, no significant differences in apoptotic cell populations were observed and in conditions analyzed, the percentage of apoptotic cells was counted less than 2% (Fig.10B).

PIM1 kinase cellular distribution is diverse. It has been found to be cytosolic, nuclear or both [2, 105]. The consequences of PIM1 subcellular localization are not yet elucidated. In cardiac explants from murine neonates and mice in the early adulthood PIM1 seems to shift from a predominantly nuclear to a more cytoplasmic localization, whereas in adults PIM1 expression is almost lost. However in a mouse model of chronic heart failure the percentage of nuclear PIM1 again markedly increased, which

was also the case in samples from failing human hearts [65]. In lymphoma cells PIM1 appeared to be predominantly nuclear, which was not the case in normal lymph nodes [89]. Irradiation promoted nuclear translocation of PIM1 in radioresistant squamocellular cancers of head and neck [106]. Taken together cellular localization seems to influence the proto-oncogenic activity of PIM kinases, possibly by substrate specificity conferred by different subcellular localization. By immunostainings of MAEC we observed an increase in endogenous nuclear PIM1 after rapamycin treatment (Fig.11B). To investigate whether the upregulation of PIM1 protein levels and the increase of its nuclear abundance were mTOR specific, we treated *Pim1*$^{+/+}$ MAEC with inhibitors of different signaling cascades. Quantification of PIM1 protein levels revealed a significant increase in PIM1 protein expression for rapamycin and AKT inhibitor IV treated cells in both, cytosol and nucleus. Also PI3K inhibition upregulated PIM1 expression levels, yet not significantly. Nevertheless, compared to untreated cells we found no significant difference in the subcellular distribution of PIM1 (cytosol vs. nucleus). Rapamycin and AKT inhibitor IV increased the whole cell PIM1 protein levels (Fig.11A).

10.2 Truncation of c-terminal residues beyond a specific Serine residue results in PIM1 nuclear translocation.

We were interested to dissect, whether overall increase in PIM1 protein levels or nuclear PIM1 alone is responsible for the significantly different proliferative response to rapamycin of *Pim1*$^{+/+}$ and *Pim1* $^{-/-}$ cells (Fig.10A and Fig.11). Ionov et al. proposed that half of the carboxy-terminus of PIM1 kinase is responsible for PIM1 nuclear translocation [89]. We performed in silico analysis to localize putative nuclear localization or export signals on the PIM1 protein sequence. However, we were not able to identify any promising sequence (data not shown).

NFATc are gene regulatory proteins, which control T-cell activation. In resting cells, they are found in the cytosol in a phosphorylated state. Upon T-cell activation, calcineurin binds to and dephosphorylates NFATc, which is then imported into the nucleus [107]. Replacement of conserved Ser residues with Ala in a Serine-rich region (SRR) of NFATc's increased their nuclear localization [108-110]. Vice versa mTOR has been shown to retain NFATc in the cytosol through basal phosphorylation

of the SRR [90]. PIM1 is known to positively influence transcriptional activity of NFATc1 on proliferation and survival [111]. Therefore we asked whether mTOR similarly regulates PIM1 cellular localization: Does PIM1 consist of an SRR, basally phosphorylated by mTOR, retaining PIM1 in the cytosol, which is abolished by mTOR inhibition through rapamycin? The PIM1 protein sequence is highly conserved in between species when comparing human, mouse, rat, bovine, frog and zebra fish sequences [89]. Sequence alignment revealed 7 Ser residues in the carboxy-terminal part, which could be putative phosphorylation targets (Fig.14). *Pim1* cDNA was truncated at these particular residues and cloned into a pdsREDT3 C1 and a pCMV-Tag 2A expression vector (Fig.12, 13). MAEC were transfected with both dsRED-*Pim1* and pCMV-Tag 2A-*Pim1* constructs. MAEC expressing dsRED-*Pim1*$^{\Delta 276-313}$ displayed a higher percentage of nuclear positive endothelial cells, which was not significant in cells expressing dsRED-*Pim1*$^{\Delta 261-313}$, but again in cells expressing dsRED-Pim1 $^{\Delta 260-313}$ and $^{\Delta 227-313}$ (Fig. 15). Overall we observed a tendency to a higher percentage of nuclear PIM1 positive cells in cells expressing PIM1 truncated beyond Ser276. However, MAEC transfected with FLAG-*Pim1*, displayed an almost complete nuclear localization of PIM1 truncated beyond Ser 276 (Fig.16). Even though the results in both experiments were not completely congruent, there seems to be a critical site for PIM1 nuclear localization around Ser 276. We further performed site directed mutagenesis of Ser 276, Ser 227, Ser 261 and Ser 261/276 to Alanine or Glutamic acid, to mimic a phospho– and dephosphorylated state (data not shown). We could not observe such consistent results as for the truncation mutants. Possible explanations could be a more complex phosphorylation pattern, which includes other Serines also, or that there are still unknown motifs, which regulate the subcellular localization of PIM1. However phopshoproteomics could help to further investigate, whether there is a phosphorylation motif, which causes cytosolic retention or nuclear translocation. Another more likely explanation could be, that mTOR inhibition activates a parallel mitogenic signalling mechanism, which counteracts rapamycin treatment by upregulation of PIM1 protein expression.

10.3 Nuclear PIM1 increases endothelial cell proliferation.

To dissect whether nuclear PIM1 affects endothelial proliferation, FLAG-*Pim1*^{wt} and FLAG-*Pim1*$^{\Delta 276-313}$ were re-expressed in *Pim1*$^{-/-}$ cells and proliferation was measured (Fig. 17C). Indeed, MAEC expressing FLAG-*Pim1*$^{\Delta 276-313}$ were more proliferative than cells transfected with FLAG-*Pim1*^{wt}. This finding could possibly explain, the fact that *Pim1*$^{-/-}$ endothelial cell proliferation is more sensitive to rapamycin than the wildtype cell proliferation.

10.4 Hypothesis

Our results show that *Pim1*$^{-/-}$ endothelial cells are more sensitive to rapamycin in terms of proliferation. Furthermore we found an increase in PIM1 protein expression levels and thereby in nuclear PIM1 protein by inhibition of key proteins of the mTOR pathway, AKT and mTOR. Re-expression of c-terminally truncated *Pim1*, which located to the nucleus, markedly increased endothelial cell proliferation.

Fig.25 shows a hypothetical model resulting from our observations. Through inhibition of the mTOR pathway by Akt inhibitor IV and rapamycin, endothelial

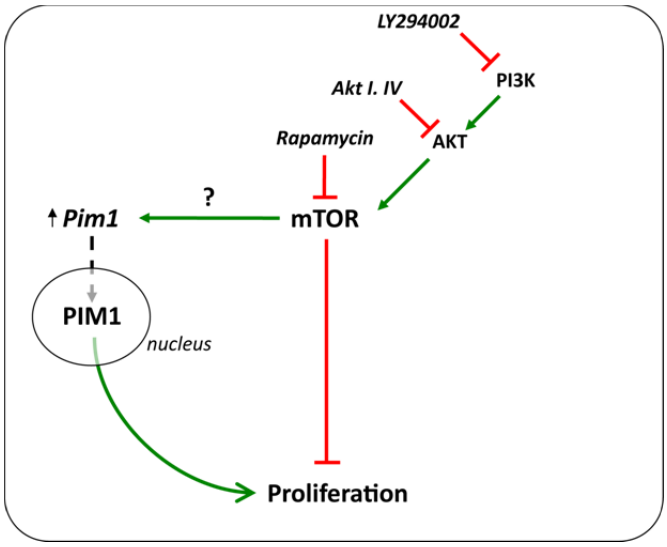

Figure 25. Hypothetical model of the regulation of PIM1 through inhibition of the mTOR pathway.

proliferation decreases. A mechanism that has not been observed so far, then leads to increased PIM1 protein levels. Mechanistically this could be at the transcriptional,

posttranscriptional, translational or posttranslational level [112, 113]. PIM1 protein levels increase in the cytosol and actively regulated or passively also nuclear PIM1 protein levels increase. Finally, as we show, especially nuclear PIM1 seemed to increase proliferation, which would explain the enhanced resistance to rapamycin of *Pim1*$^{+/+}$ cells.

10.5 PIM1 function in the nucleus

Nuclear PIM1 has been associated with resistance to cancer treatment, but little is known about the interactions of PIM1 in the nucleus. PIM1 has been shown to promote cell cycle progression by phosphorylation of the cell cycle inhibitors p27^{Kip1} and p21$^{Cip1/WAF1}$ [77, 78]. p27^{Kip1} phosphorylation induced cytoplasmic localization and subsequent proteasomal degradation of the cyclin-dependent-kinase inhibitor. p21$^{Cip1/WAF1}$ also localizes to the cytoplasm, once phosphorylated by PIM1 kinase. Also c-MYC has been shown to cooperate with PIM1 in cell cycle progression and cell tumorigenesis [114-116]. However, only decades later additional mechanistic insight of this interaction was provided: In the nucleus, PIM1 phosphorylates histone H3 in HUVEC's, which leads to MYC-driven transcription and cell transformation [117]. It has also been suggested that PIM1 phosphorylates heterochromatin protein 1, a histone H3 binding transcriptional repressor, reducing its gene silencing function [118]. Additionally PIM1 appeared to be nuclear in radioresistant tumors [106] and the pathologically challenged myocard [65]. Interestingly preliminary data indicates, that in cells treated with rapamycin, we observe that dsRED-*Pim1*^{wt} localizes in foci at the intersection of eu- and heterochromatin (data not shown). At these sites where active transcription takes place, many signaling kinases, such as PKB/AKT, S6K1 or JNK1, shuttle to the nucleus where they modify histones and influence the condensation state and thereby the transcriptional accessibilty of chromatin [119].
We speculate, that PIM1 may elicite its regulatory function in the cell nucleus through epigenetic regulation. The existence of such a PIM1-dependent transcriptional regulation is supported by data obtained from gene expression profiling of *Pim1* wildtype and *Pim1*$^{-/-}$ cells: The vast number (1598) of significantly (P<0.01) regulated genes when comparing wildtype and *Pim1*$^{-/-}$ MAECs found by gene expression profiling, suggests a more general rather than transcription factor-dependent type of

regulation mediated by PIM1 (see section 6.2.6). In cancer, aberrant silencing or activation of gene expression often occurs through epigenetic regulation, which triggers abnormal cell behaviour, such as malignant transformation but also changes in adhesive properties of cells [120, 121]. Two prominent mechanisms responsible for cancer development and progression, are promoter hypermethylation, which elicits gene silencing, and histone modifications, which determines the accessibilty of the transcription machinery to chromatin [121-123]. Regulation of the key genes involved in cell adhesion, we found to have a different expression pattern comparing *Pim1*$^{-/-}$ vs. *Pim1*$^{+/+}$ cells, have been reported to be silenced by such mechanisms: The promoter of *Cdh13* in various tumors and *Jam2* in colorectal adenomas and carcinomas was found to be hypermethylated [124-126]. *Icam1* in tumor endothelial cells and *Itga7* expression in hepatoma cells has been shown to be epigenetically regulated through histone modifications [127, 128]. In the present study all these genes were found to be significantly upregulated in *Pim1*$^{-/-}$ cells (Table 5, Fig23). Nevertheless, further investigations are needed, also in cancer cell lines, to shed further light on PIM1's potential role in epigenetic regulation of cell adhesion, tumor angiogenesis and metastasis.

10.6 *Pim1* deletion increases endothelial cell adhesion and thereby affects cell motility.

In the present study we report that PIM1 plays a distinct role in endothelial cell-cell cohesion and cell-matrix adhesion. We demonstrate that *Pim1* deletion and kinase inhibition slows endothelial cell detachment by trypsinization and increases total electrical resistance across the endothelial monolayer. Reintroduction of *Pim1* cDNA into *Pim1*$^{-/-}$ cells partially but significantly restored electrical resistance to wildtype levels. Furthermore, *Pim1* deletion in endothelial cells markedly reduced cell motility as shown in wound healing assays. This finding is consistent with an earlier report using cells derived from human prostate cancer or squamo-cellular carcinoma where *Pim1* silencing decreased wound healing in vitro [75]. We therefore conclude that modulation of endothelial cell adhesion by *Pim1* deletion, kinase inhibition and *Pim1* cDNA reintroduction into *Pim1*$^{-/-}$ cells is actually *Pim1*-specific. Most likely this

requires its classical serine-threonine kinase activity, as suggested earlier by Santio et al., since a similar PIM1 kinase inhibitor in human cancer cells slowed down cell motility [75].

Cell migration is a complex, tightly regulated process that involves the dynamic formation and disassembly of distinct adhesion complexes [129, 130]. We therefore further dissected the characteristics of endothelial cell adhesion modulation by differentiating electrical resistance values and found that both cell-cell cohesion and cell-substrate adhesion were reinforced by *Pim1* deletion.

10.7 Endothelial cell-cell junctions and focal adhesion structures are more pronounced in *Pim1* knockout cells.

The intracellular domain of the adherens junctions effector protein VE–cadherin contains a distal binding site for β-catenin. β-catenin is linked to α-catenin, which may further interact with the cytoskeleton via α-actinin and vinculin [30, 97]. Finally, integrins directly adhere to the matrix substratum and connect to talin and vinculin, [131]. Interestingly, *Pim1*$^{-/-}$ cells exhibited more vinculin positive focal adhesion structures that spread throughout the entire endothelial cell surface, whereas wildtype cells displayed less vinculin positive streaks that were predominantly located laterally at cell junctions. Furthermore, *Pim1*$^{-/-}$ cells displayed abnormally enlarged β-catenin positive structures at cell-cell junctions than usually found in wildtype endothelial cells. Thus, *Pim1* deletion reinforced connection complexes between cell-to-cell junctions and focal adhesion structures, which might mechanically increase intercellular forces and tension [132]. While *Pim1* deletion did not change overall β-catenin and vinculin protein levels, gene expression analysis demonstrated significant and strong regulation of matrix components (*Col6a, Col11a*) and cell to matrix (*Itga7*) and cell-to-cell attachment (*Cdh13, Jam2*) modulating genes. MetaCore™ analysis of all genes modulated by *Pim1* deletion revealed WNT-mediated cytoskeleton remodeling as the most significantly regulated biological process.

10.8 *Pim1* knockout-deposited matrix induces adhesion characteristics of *Pim1* knockout cells in wildtype cells.

Pim1$^{-/-}$ but not wildtype cells deposited a specific, COL6A3-containing matrix in fibre-like structures on culture dish surfaces: Intriguingly, ECM deposited by *Pim1*$^{-/-}$ cells alone was sufficient to induce *Pim1*$^{-/-}$ adhesion characteristics in wildtype cells, with respect to cell detachment and adherens junction strengthening. This may be interpreted as one of the early events in the establishment of the *Pim1*$^{-/-}$ adhesion phenotype. Matrix-integrin mediated signals are transduced by the focal adhesion kinase (FAK) [30]. Thus, enhanced matrix-integrin interactions in *Pim1*$^{-/-}$ cells may increase vinculin-containing focal adhesion structures and modulate FAK signaling. Observations in different model systems suggest a complex and dynamic cross talk between the focal adhesion kinase and the WNT-signaling pathway [133, 134]. Canonical WNT-signalling promotes dissociation of β-catenin from junctional complexes to the nucleus, which also results in reduced cell-cell adhesion in tumorigenesis [23]. As we show in Fig. 5B, *Pim1*$^{-/-}$ MAEC display pronounced β-catenin clusters at the cell to cell borders, which could be hypothetically explained by reduced WNT-signalling in these cells. This is also demonstrated in FAK kinase dead mutant mice where vascular permeability and angiogenic growth factor VEGF failed to induce dissociation of β-catenin from adherens junction complexes [135]. Intriguingly we found that *Pim1*$^{-/-}$ cell-deposited matrix also enhanced β-catenin-containing structures at cell-cell contacts of wildtype MAEC. Therefore, we assume that matrix- induced signalling may repress WNT signaling in *Pim1*$^{-/-}$ endothelium preventing redistribution of β-catenin from adherens junctions to the nucleus, thereby enhancing cell-cell cohesion.

10.9 Conclusion

Taken together, we demonstrate two distinct novel roles for PIM1 in endothelial cells. First, we show that Pim1 causes endothelial proliferation to be more sensitive to rapamycin. In wildtype cells we show that rapamycin treatment leads to an increase in PIM1 protein levels in the cytosol and the nucleus. By transfection of different c-terminal truncations of PIM1 we found a region around Ser276 to be critical for

nuclear localization of the kinase. Re-expression of this truncation mutant in *Pim1*$^{-/-}$ cells significantly increased proliferation compared to cells expressing wildtype *Pim1*. Additionally, preliminary data indicates that this effect is rapamycin insensitive. We conclude that PIM1 nuclear abundance increases endothelial cell proliferation, in an at least partially rapamycin independent way. Therefore, PIM1 kinase inhibitors might be useful angiogenic inhibitors in combination with rapalogues. Especially in cancer known to be positively stimulated by PIM1, or in cancer insensitive to rapamycin. Furthermore the subcellular localization of PIM1 could be a prognostic marker for tumor progression and drug response.

Second, we show a novel role of PIM1 in the regulation of endothelial cell-cell cohesion and cell-matrix adhesion, which likely involves a matrix-initiated response, involving collagen, alteration in vinculin-containing focal adhesion structures and pronounced β-catenin-containing junctional complexes. This is accompanied by alterations in cell adhesion gene regulation. A hyperadhesive endothelial *Pim1*$^{-/-}$ phenotype might be useful to promote endothelial barrier integrity, restrict angiogenesis in growing tumors and impede invasion and metastatic spread of malignant cells through the endothelial monolayer.

11 Acknowledgments

I owe many thanks. The first of these to Prof. Dr. Edouard J. Battegay for giving me the opportunity to carry out my thesis in his laboratory.You always encouraged me to work creatively and gave me good advice.

Special thanks go to Dr. Rok Humar who gave me guidance for my work, scientific support, intensive discussions about and beside work and for being a friend.

I am indebted to Prof. Dr. Roland H. Wenger who accepted to be the chairman of my PhD committee and for giving me helpful advice. I also thank Prof. Dr. Michael N. Hall who accepted to be a member of my PhD committee. Furthermore, I thank Prof. Dr. Martin Pruschy who accepted to be a faculty representative for the thesis defense and Prof. Dr. Thérèse J. Resink to write an external eypertise.

I thank Dr. Elvira Haas for fruitful discussions and helpful scientific support.

I thank Prof. Juerg Schwaller without whom I would not know PIM. Thank you for support and helpful advice.

Many thanks to all former and present lab members and the administrative staff of the laboratory. By name Claudia Weiss, Mirjam Sollberger, Marco Petrimpol, Lourdes Sanchez de Miguel, Sonja Jakob, Ana Perez, Valia Georgiopoulou, Fabio Aimi, Katja Drägert and also Hartmut Berns for the Rechenlineal.

I am thankful to Indranil Bhattacharya and Marlen Damjanovic, who helped to make it worth to come to Zürich.

I also thank Dr. Ina Kalus, who always helped me, scientifically or beyond, for nice coffee breaks and for friendship.

Special thanks go to Martin Peier, to become a friend, for support and a really nice time. Misery loves company!

I am thankful to all my friends who made my life easier outside of work. (Merci Zipfla)

Last but not least I am deeply greatful to my father for his patience and support. I am thankful also to my sister and my brother for being there in good times and in bad.

12 SUPPLEMENTARY MATERIAL TABLES

Gene Symbol	Sequence (5'-3')
Itga3	FWD TGTGTACCTGTGTCCCCTCA
	REV CTTCTAGCCCAGACCACAGC
Itgb4	FWD ATCTGGGAAGATGGGAGGAG
	REV CAGGAGGGTGCTGCTGACT
Itga7	FWD ACTGGAAGGGGTTGCTTTTT
	REV CTGAGCGCATAAGACCCTTC
Itga11	FWD CGCCTTCCTCTGCTTCATAC
	REV GGCTCTGTTGGTGAACTGGT
Jam2	FWD GGGAAGCGAATGCAAGTAGA
	REV GCCCTTCTGGAAGGAAGTTT
Icam1	FWD TTCACACTGAATGCCAGCTC
	REV GTCTGCTGAGACCCCTCTTG
Vcam1	FWD ACAGACAGTCCCCTCAATGG
	REV ACCTCCACCTGGGTTCTCTT
Cdh13	FWD TGCTGAAGACATGGCAGAAC
	REV GGCTGTCTCTGGTTCTCTGG
Col6a3	FWD AGACCAAGAGGAGCTGGTGA
	REV AAGGGGGATATCGGGTACTG
Col11a1	FWD CTGGTCATCCTGGGAAAGAA
	REV ACCCTTTTCGCCTTTAGAGC
Svep1	FWD GCTCCATAAGCCAGCTCAAC
	REV CGGACAATCAGAGCAGAACA
Adam23	FWD CTACAATGGCGAGTGCAAGA
	REV TGCAAAGCAGAAATCCACAG
Pim1	FWD GGCGAAATCAAACTCATCGA
	REV CCGGTGACAGACTGTGCAGAT
Gapdh	FWD AAA TGG TGA AGG TCG GTG TG
	REV GTT GAA TTT GCC GTG AGT GG
FLAG-Pim1	FWD GATTACAAGGATGACGACGATAAGGCCCGG
	REV CTGCAGCCCGGGGGATCCGC

Supplementary material table S1. Primer list of primers used for the validation of the microarray.

Gene Symbol	Sequence (5'-3')
Pim1 Δ 312-313	FWD GCTGATGGTCGACCTAGGGCCCCGGCGACAGGC
	REV CTCGAGTGCCCATGGAAGTG
Pim1 Δ 308-313	FWD GCTGATGGTCGACCTACAGGCTGTGGAGGTGGATC
	REV CTCGAGTGCCCATGGAAGTG
Pim1 Δ 306-313	FWD CTGATGGTCGACCTAGTGGAGGTGGATCTCAGCAG
	REV CTCGAGTGCCCATGGAAGTG
Pim1 Δ 276-313	FWD GCTGATGGTCGACCTATGGTCTCAGGGCCAAGCAC
	REV CTCGAGTGCCCATGGAAGTG
Pim1 Δ 261-313	FWD GCTGATGGTCGACCTAAGAGACCCTCTGCCTGAAG
	REV CTCGAGTGCCCATGGAAGTG
Pim1 Δ 260-313	FWD GATGGTCGACCTAGACCCTCTGCCTGAAGAAAACC
	REV CTCGAGTGCCCATGGAAGTG
Pim1 Δ 227-313	FWD GCTGATGGTCGACCTACCAGACTGCCGCCGACCTG
	REV CTCGAGTGCCCATGGAAGTG

Supplementary material table S2. Primer list for the generation of the truncation mutants

13 REFERENCES

1. Mikkers, H., et al., *Mice deficient for all PIM kinases display reduced body size and impaired responses to hematopoietic growth factors.* Mol Cell Biol, 2004. **24**(13): p. 6104-15.

2. Xie, Y., et al., *The 44 kDa Pim-1 kinase directly interacts with tyrosine kinase Etk/BMX and protects human prostate cancer cells from apoptosis induced by chemotherapeutic drugs.* Oncogene, 2006. **25**(1): p. 70-8.

3. Aumüller, G., G. Aust, and L.J. Wurzinger, *Anatomie*. 2006: Thieme.

4. Foster, K.G. and D.C. Fingar, *Mammalian target of rapamycin (mTOR): conducting the cellular signaling symphony.* J Biol Chem, 2010. **285**(19): p. 14071-7.

5. Stavropoulou, V., L. Brault, and J. Schwaller, *Insights into molecular pathways for targeted therapeutics in acute leukemia.* Swiss Med Wkly, 2010. **140**: p. w13068.

6. Fox, C.J., P.S. Hammerman, and C.B. Thompson, *Fuel feeds function: energy metabolism and the T-cell response.* Nat Rev Immunol, 2005. **5**(11): p. 844-52.

7. Francavilla, C., L. Maddaluno, and U. Cavallaro, *The functional role of cell adhesion molecules in tumor angiogenesis.* Semin Cancer Biol, 2009. **19**(5): p. 298-309.

8. Helmlinger, G., et al., *Interstitial pH and pO2 gradients in solid tumors in vivo: high-resolution measurements reveal a lack of correlation.* Nat Med, 1997. **3**(2): p. 177-82.

9. Carmeliet, P. and R.K. Jain, *Angiogenesis in cancer and other diseases.* Nature, 2000. **407**(6801): p. 249-57.

10. Nawijn, M.C., A. Alendar, and A. Berns, *For better or for worse: the role of Pim oncogenes in tumorigenesis.* Nat Rev Cancer, 2011. **11**(1): p. 23-34.

11. Vestweber, D., *Molecular mechanisms that control endothelial cell contacts.* J Pathol, 2000. **190**(3): p. 281-91.

12. Vandenbroucke, E., et al., *Regulation of endothelial junctional permeability.* Ann N Y Acad Sci, 2008. **1123**: p. 134-45.

13. Komarova, Y. and A.B. Malik, *Regulation of endothelial permeability via paracellular and transcellular transport pathways.* Annu Rev Physiol, 2010. **72**: p. 463-93.

14. Tuma, P.L. and A.L. Hubbard, *Transcytosis: crossing cellular barriers.* Physiol Rev, 2003. **83**(3): p. 871-932.

15. Martin, T.A. and W.G. Jiang, *Loss of tight junction barrier function and its role in cancer metastasis.* Biochim Biophys Acta, 2009. **1788**(4): p. 872-91.

16. Carmeliet, P., et al., *Targeted deficiency or cytosolic truncation of the VE-cadherin gene in mice impairs VEGF-mediated endothelial survival and angiogenesis.* Cell, 1999. **98**(2): p. 147-57.

17. Abraham, S., et al., *VE-Cadherin-mediated cell-cell interaction suppresses sprouting via signaling to MLC2 phosphorylation.* Curr Biol, 2009. **19**(8): p. 668-74.

18. Grazia Lampugnani, M., et al., *Contact inhibition of VEGF-induced proliferation requires vascular endothelial cadherin, beta-catenin, and the phosphatase DEP-1/CD148.* J Cell Biol, 2003. **161**(4): p. 793-804.

19. Patel, S.D., et al., *Cadherin-mediated cell-cell adhesion: sticking together as a family.* Curr Opin Struct Biol, 2003. **13**(6): p. 690-8.

20. Vincent, P.A., et al., *VE-cadherin: adhesion at arm's length.* Am J Physiol Cell Physiol, 2004. **286**(5): p. C987-97.

21. Boggon, T.J., et al., *C-cadherin ectodomain structure and implications for cell adhesion mechanisms.* Science, 2002. **296**(5571): p. 1308-13.

22. Shapiro, L. and W.I. Weis, *Structure and biochemistry of cadherins and catenins.* Cold Spring Harb Perspect Biol, 2009. **1**(3): p. a003053.

23. Fu, Y., et al., *beta-catenin as a potential key target for tumor suppression.* Int J Cancer, 2011. **129**(7): p. 1541-51.

24. Zerlin, M., M.A. Julius, and J. Kitajewski, *Wnt/Frizzled signaling in angiogenesis.* Angiogenesis, 2008. **11**(1): p. 63-9.

25. Dejana, E., F. Orsenigo, and M.G. Lampugnani, *The role of adherens junctions and VE-cadherin in the control of vascular permeability.* J Cell Sci, 2008. **121**(Pt 13): p. 2115-22.

26. Drees, F., et al., *Alpha-catenin is a molecular switch that binds E-cadherin-beta-catenin and regulates actin-filament assembly.* Cell, 2005. **123**(5): p. 903-15.

27. Zhao, X. and J.L. Guan, *Focal adhesion kinase and its signaling pathways in cell migration and angiogenesis.* Adv Drug Deliv Rev, 2011. **63**(8): p. 610-5.

28. Hynes, R.O., *Integrins: bidirectional, allosteric signaling machines.* Cell, 2002. **110**(6): p. 673-87.

29. Brakebusch, C. and R. Fassler, *The integrin-actin connection, an eternal love affair.* EMBO J, 2003. **22**(10): p. 2324-33.

30. Quadri, S.K., *Cross talk between focal adhesion kinase and cadherins: role in regulating endothelial barrier function.* Microvasc Res, 2012. **83**(1): p. 3-11.

31. Carmeliet, P., *Angiogenesis in life, disease and medicine.* Nature, 2005. **438**(7070): p. 932-6.

32. Augustin, H.G., et al., *Control of vascular morphogenesis and homeostasis through the angiopoietin-Tie system.* Nat Rev Mol Cell Biol, 2009. **10**(3): p. 165-77.

33. van Hinsbergh, V.W. and P. Koolwijk, *Endothelial sprouting and angiogenesis: matrix metalloproteinases in the lead.* Cardiovasc Res, 2008. **78**(2): p. 203-12.

34. Rundhaug, J.E., *Matrix metalloproteinases and angiogenesis.* J Cell Mol Med, 2005. **9**(2): p. 267-85.

35. Chung, A.S., J. Lee, and N. Ferrara, *Targeting the tumour vasculature: insights from physiological angiogenesis.* Nat Rev Cancer, 2010. **10**(7): p. 505-14.

36. Carmeliet, P., *Angiogenesis in health and disease.* Nat Med, 2003. **9**(6): p. 653-60.

37. Bergers, G. and L.E. Benjamin, *Tumorigenesis and the angiogenic switch.* Nat Rev Cancer, 2003. **3**(6): p. 401-10.

38. Nagy, J.A., et al., *Why are tumour blood vessels abnormal and why is it important to know?* Br J Cancer, 2009. **100**(6): p. 865-9.

39. Weis, S., et al., *Endothelial barrier disruption by VEGF-mediated Src activity potentiates tumor cell extravasation and metastasis.* J Cell Biol, 2004. **167**(2): p. 223-9.

40. Vezina, C., A. Kudelski, and S.N. Sehgal, *Rapamycin (AY-22,989), a new antifungal antibiotic. I. Taxonomy of the producing streptomycete and isolation of the active principle.* J Antibiot (Tokyo), 1975. **28**(10): p. 721-6.

41. Heitman, J., N.R. Movva, and M.N. Hall, *Targets for cell cycle arrest by the immunosuppressant rapamycin in yeast.* Science, 1991. **253**(5022): p. 905-9.

42. Brown, E.J., et al., *A mammalian protein targeted by G1-arresting rapamycin-receptor complex.* Nature, 1994. **369**(6483): p. 756-8.

43. Sabatini, D.M., et al., *RAFT1: a mammalian protein that binds to FKBP12 in a rapamycin-dependent fashion and is homologous to yeast TORs.* Cell, 1994. **78**(1): p. 35-43.

44. Chen, Y., et al., *A putative sirolimus (rapamycin) effector protein.* Biochem Biophys Res Commun, 1994. **203**(1): p. 1-7.

45. Chiu, M.I., H. Katz, and V. Berlin, *RAPT1, a mammalian homolog of yeast Tor, interacts with the FKBP12/rapamycin complex.* Proc Natl Acad Sci U S A, 1994. **91**(26): p. 12574-8.

46. Sabers, C.J., et al., *Isolation of a protein target of the FKBP12-rapamycin complex in mammalian cells.* J Biol Chem, 1995. **270**(2): p. 815-22.

47. Guertin, D.A., et al., *Ablation in mice of the mTORC components raptor, rictor, or mLST8 reveals that mTORC2 is required for signaling to Akt-FOXO and PKCalpha, but not S6K1.* Dev Cell, 2006. **11**(6): p. 859-71.

48. Zoncu, R., A. Efeyan, and D.M. Sabatini, *mTOR: from growth signal integration to cancer, diabetes and ageing.* Nat Rev Mol Cell Biol, 2011. **12**(1): p. 21-35.

49. Pearce, L.R., et al., *Identification of Protor as a novel Rictor-binding component of mTOR complex-2.* Biochem J, 2007. **405**(3): p. 513-22.

50. Sarbassov, D.D., et al., *Prolonged rapamycin treatment inhibits mTORC2 assembly and Akt/PKB.* Mol Cell, 2006. **22**(2): p. 159-68.

51. Laplante, M. and D.M. Sabatini, *mTOR signaling in growth control and disease.* Cell, 2012. **149**(2): p. 274-93.

52. Wullschleger, S., R. Loewith, and M.N. Hall, *TOR signaling in growth and metabolism.* Cell, 2006. **124**(3): p. 471-84.

53. Dunlop, E.A. and A.R. Tee, *Mammalian target of rapamycin complex 1: signalling inputs, substrates and feedback mechanisms.* Cell Signal, 2009. **21**(6): p. 827-35.

54. Ma, X.M. and J. Blenis, *Molecular mechanisms of mTOR-mediated translational control.* Nat Rev Mol Cell Biol, 2009. **10**(5): p. 307-18.

55. Harrington, L.S., et al., *The TSC1-2 tumor suppressor controls insulin-PI3K signaling via regulation of IRS proteins.* J Cell Biol, 2004. **166**(2): p. 213-23.

56. Sarbassov, D.D., et al., *Phosphorylation and regulation of Akt/PKB by the rictor-mTOR complex.* Science, 2005. **307**(5712): p. 1098-101.

57. Zinzalla, V., et al., *Activation of mTORC2 by association with the ribosome.* Cell, 2011. **144**(5): p. 757-68.

58. Bhaskar, P.T. and N. Hay, *The two TORCs and Akt.* Dev Cell, 2007. **12**(4): p. 487-502.

59. Qian, K.C., et al., *Structural basis of constitutive activity and a unique nucleotide binding mode of human Pim-1 kinase.* J Biol Chem, 2005. **280**(7): p. 6130-7.

60. Breuer, M.L., H.T. Cuypers, and A. Berns, *Evidence for the involvement of pim-2, a new common proviral insertion site, in progression of lymphomas.* EMBO J, 1989. **8**(3): p. 743-8.

61. Feldman, J.D., et al., *KID-1, a protein kinase induced by depolarization in brain.* J Biol Chem, 1998. **273**(26): p. 16535-43.

62. van der Lugt, N.M., et al., *Proviral tagging in E mu-myc transgenic mice lacking the Pim-1 proto-oncogene leads to compensatory activation of Pim-2.* EMBO J, 1995. **14**(11): p. 2536-44.

63. Katakami, N., et al., *Role of pim-1 in smooth muscle cell proliferation.* J Biol Chem, 2004. **279**(52): p. 54742-9.

64. Laird, P.W., et al., *In vivo analysis of Pim-1 deficiency.* Nucleic Acids Res, 1993. **21**(20): p. 4750-5.

65. Muraski, J.A., et al., *Pim-1 regulates cardiomyocyte survival downstream of Akt.* Nat Med, 2007. **13**(12): p. 1467-75.

66. Zippo, A., et al., *Identification of Flk-1 target genes in vasculogenesis: Pim-1 is required for endothelial and mural cell differentiation in vitro.* Blood, 2004. **103**(12): p. 4536-44.

67. Castro, A., et al., *IL-4 selectively inhibits IL-2-triggered Stat5 activation, but not proliferation, in human T cells.* J Immunol, 1999. **162**(3): p. 1261-9.

68. Shirogane, T., et al., *Synergistic roles for Pim-1 and c-Myc in STAT3-mediated cell cycle progression and antiapoptosis.* Immunity, 1999. **11**(6): p. 709-19.

69. Wright, G., et al., *A gene expression-based method to diagnose clinically distinct subgroups of diffuse large B cell lymphoma.* Proc Natl Acad Sci U S A, 2003. **100**(17): p. 9991-6.

70. de Vos, S., et al., *Cell cycle alterations in the blastoid variant of mantle cell lymphoma (MCL-BV) as detected by gene expression profiling of mantle cell lymphoma (MCL) and MCL-BV.* Diagn Mol Pathol, 2003. **12**(1): p. 35-43.

71. Reiser-Erkan, C., et al., *Hypoxia-inducible proto-oncogene Pim-1 is a prognostic marker in pancreatic ductal adenocarcinoma.* Cancer Biol Ther, 2008. **7**(9): p. 1352-9.

72. Warnecke-Eberz, U., et al., *Frequent down-regulation of pim-1 mRNA expression in non-small cell lung cancer is associated with lymph node metastases.* Oncol Rep, 2008. **20**(3): p. 619-24.

73. Tanaka, S., et al., *Pim-1 activation of cell motility induces the malignant phenotype of tongue carcinoma.* Mol Med Report, 2009. **2**(2): p. 313-8.

74. Warnecke-Eberz, U., et al., *Prognostic impact of protein overexpression of the proto-oncogene PIM-1 in gastric cancer.* Anticancer Res, 2009. **29**(11): p. 4451-5.

75. Santio, N.M., et al., *Pim-selective inhibitor DHPCC-9 reveals Pim kinases as potent stimulators of cancer cell migration and invasion.* Mol Cancer, 2010. **9**: p. 279.

76. Brault, L., et al., *PIM serine/threonine kinases in the pathogenesis and therapy of hematologic malignancies and solid cancers.* Haematologica, 2010. **95**(6): p. 1004-15.

77. Morishita, D., et al., *Pim kinases promote cell cycle progression by phosphorylating and down-regulating p27Kip1 at the transcriptional and posttranscriptional levels.* Cancer Res, 2008. **68**(13): p. 5076-85.

78. Wang, Z., et al., *Phosphorylation of the cell cycle inhibitor p21Cip1/WAF1 by Pim-1 kinase.* Biochim Biophys Acta, 2002. **1593**(1): p. 45-55.

79. Bachmann, M., et al., *The oncogenic serine/threonine kinase Pim-1 phosphorylates and inhibits the activity of Cdc25C-associated kinase 1 (C-TAK1): a novel role for Pim-1 at the G2/M cell cycle checkpoint.* J Biol Chem, 2004. **279**(46): p. 48319-28.

80. Peltola, K.J., et al., *Pim-1 kinase inhibits STAT5-dependent transcription via its interactions with SOCS1 and SOCS3.* Blood, 2004. **103**(10): p. 3744-50.

81. Aho, T.L., et al., *Pim-1 kinase promotes inactivation of the pro-apoptotic Bad protein by phosphorylating it on the Ser112 gatekeeper site.* FEBS Lett, 2004. **571**(1-3): p. 43-9.

82. Grundler, R., et al., *Dissection of PIM serine/threonine kinases in FLT3-ITD-induced leukemogenesis reveals PIM1 as regulator of CXCL12-CXCR4-mediated homing and migration.* J Exp Med, 2009. **206**(9): p. 1957-70.

83. Fox, C.J., P.S. Hammerman, and C.B. Thompson, *The Pim kinases control rapamycin-resistant T cell survival and activation.* J Exp Med, 2005. **201**(2): p. 259-66.

84. Schatz, J.H., et al., *Targeting cap-dependent translation blocks converging survival signals by AKT and PIM kinases in lymphoma.* J Exp Med, 2011. **208**(9): p. 1799-807.

85. Zhang, F., et al., *PIM1 protein kinase regulates PRAS40 phosphorylation and mTOR activity in FDCP1 cells.* Cancer Biol Ther, 2009. **8**(9): p. 846-53.

86. Humar, R., et al., *Hypoxia enhances vascular cell proliferation and angiogenesis in vitro via rapamycin (mTOR)-dependent signaling.* FASEB J, 2002. **16**(8): p. 771-80.

87. Li, W., et al., *Hypoxia-induced endothelial proliferation requires both mTORC1 and mTORC2.* Circ Res, 2007. **100**(1): p. 79-87.

88. Schmittgen, T.D., et al., *Real-time PCR quantification of precursor and mature microRNA.* Methods, 2008. **44**(1): p. 31-8.

89. Ionov, Y., et al., *Pim-1 protein kinase is nuclear in Burkitt's lymphoma: nuclear localization is necessary for its biologic effects.* Anticancer Res, 2003. **23**(1A): p. 167-78.

90. Yang, T.T., et al., *Integration of protein kinases mTOR and extracellular signal-regulated kinase 5 in regulating nucleocytoplasmic localization of NFATc4.* Mol Cell Biol, 2008. **28**(10): p. 3489-501.

91. Al-Mehdi, A.B., et al., *Intravascular origin of metastasis from the proliferation of endothelium-attached tumor cells: a new model for metastasis.* Nat Med, 2000. **6**(1): p. 100-2.

92. Teicher, B.A. and S.P. Fricker, *CXCL12 (SDF-1)/CXCR4 pathway in cancer.* Clin Cancer Res, 2010. **16**(11): p. 2927-31.

93. Pogacic, V., et al., *Structural analysis identifies imidazo[1,2-b]pyridazines as PIM kinase inhibitors with in vitro antileukemic activity.* Cancer Res, 2007. **67**(14): p. 6916-24.

94. Giaever, I. and C.R. Keese, *Micromotion of mammalian cells measured electrically.* Proc Natl Acad Sci U S A, 1991. **88**(17): p. 7896-900.

95. Bagnaninchi, P.O. and N. Drummond, *Real-time label-free monitoring of adipose-derived stem cell differentiation with electric cell-substrate impedance sensing.* Proc Natl Acad Sci U S A, 2011. **108**(16): p. 6462-7.

96. Nyqvist, D., C. Giampietro, and E. Dejana, *Deciphering the functional role of endothelial junctions by using in vivo models.* EMBO Rep, 2008. **9**(8): p. 742-7.

97. Wallez, Y. and P. Huber, *Endothelial adherens and tight junctions in vascular homeostasis, inflammation and angiogenesis.* Biochim Biophys Acta, 2008. **1778**(3): p. 794-809.

98. Shefer, G. and D. Benayahu, *SVEP1 is a novel marker of activated pre-determined skeletal muscle satellite cells.* Stem Cell Rev, 2010. **6**(1): p. 42-9.

99. Costa, P. and M. Parsons, *New insights into the dynamics of cell adhesions.* Int Rev Cell Mol Biol, 2010. **283**: p. 57-91.

100. Merkel, A.L., E. Meggers, and M. Ocker, *PIM1 kinase as a target for cancer therapy.* Expert Opin Investig Drugs, 2012. **21**(4): p. 425-36.

101. Gabardi, S. and S.A. Baroletti, *Everolimus: a proliferation signal inhibitor with clinical applications in organ transplantation, oncology, and cardiology.* Pharmacotherapy, 2010. **30**(10): p. 1044-56.

102. Guba, M., et al., *Rapamycin inhibits primary and metastatic tumor growth by antiangiogenesis: involvement of vascular endothelial growth factor.* Nat Med, 2002. **8**(2): p. 128-35.

103. Benjamin, D., et al., *Rapamycin passes the torch: a new generation of mTOR inhibitors.* Nat Rev Drug Discov, 2011. **10**(11): p. 868-80.

104. Song, J.H. and A.S. Kraft, *Pim kinase inhibitors sensitize prostate cancer cells to apoptosis triggered by Bcl-2 family inhibitor ABT-737.* Cancer Res, 2012. **72**(1): p. 294-303.

105. Brault, L., et al., *PIM kinases are progression markers and emerging therapeutic targets in diffuse large B-cell lymphoma.* Br J Cancer, 2012.

106. Peltola, K., et al., *Pim-1 kinase expression predicts radiation response in squamocellular carcinoma of head and neck and is under the control of epidermal growth factor receptor.* Neoplasia, 2009. **11**(7): p. 629-36.

107. Li, H., A. Rao, and P.G. Hogan, *Interaction of calcineurin with substrates and targeting proteins.* Trends Cell Biol, 2011. **21**(2): p. 91-103.

108. Chow, C.W., et al., *c-Jun NH(2)-terminal kinase inhibits targeting of the protein phosphatase calcineurin to NFATc1.* Mol Cell Biol, 2000. **20**(14): p. 5227-34.

109. Chow, C.W., et al., *Nuclear accumulation of NFAT4 opposed by the JNK signal transduction pathway.* Science, 1997. **278**(5343): p. 1638-41.

110. Yang, T.T., et al., *Phosphorylation of NFATc4 by p38 mitogen-activated protein kinases.* Mol Cell Biol, 2002. **22**(11): p. 3892-904.

111. Rainio, E.M., J. Sandholm, and P.J. Koskinen, *Cutting edge: Transcriptional activity of NFATc1 is enhanced by the Pim-1 kinase.* J Immunol, 2002. **168**(4): p. 1524-7.

112. Hoover, D.S., et al., *Pim-1 protein expression is regulated by its 5'-untranslated region and translation initiation factor eIF-4E.* Cell Growth Differ, 1997. **8**(12): p. 1371-80.

113. Shay, K.P., et al., *Pim-1 kinase stability is regulated by heat shock proteins and the ubiquitin-proteasome pathway.* Mol Cancer Res, 2005. **3**(3): p. 170-81.

114. van Lohuizen, M., et al., *Predisposition to lymphomagenesis in pim-1 transgenic mice: cooperation with c-myc and N-myc in murine leukemia virus-induced tumors.* Cell, 1989. **56**(4): p. 673-82.

115. van Lohuizen, M., et al., *Identification of cooperating oncogenes in E mu-myc transgenic mice by provirus tagging.* Cell, 1991. **65**(5): p. 737-52.

116. Verbeek, S., et al., *Mice bearing the E mu-myc and E mu-pim-1 transgenes develop pre-B-cell leukemia prenatally.* Mol Cell Biol, 1991. **11**(2): p. 1176-9.

117. Zippo, A., et al., *PIM1-dependent phosphorylation of histone H3 at serine 10 is required for MYC-dependent transcriptional activation and oncogenic transformation.* Nat Cell Biol, 2007. **9**(8): p. 932-44.

118. Koike, N., et al., *Identification of heterochromatin protein 1 (HP1) as a phosphorylation target by Pim-1 kinase and the effect of phosphorylation on the transcriptional repression function of HP1(1).* FEBS Lett, 2000. **467**(1): p. 17-21.

119. Baek, S.H., *When signaling kinases meet histones and histone modifiers in the nucleus.* Mol Cell, 2011. **42**(3): p. 274-84.

120. Esteller, M., *CpG island hypermethylation and tumor suppressor genes: a booming present, a brighter future.* Oncogene, 2002. **21**(35): p. 5427-40.

121. Rodriguez-Paredes, M. and M. Esteller, *Cancer epigenetics reaches mainstream oncology.* Nat Med, 2011. **17**(3): p. 330-9.

122. Berger, S.L., *The complex language of chromatin regulation during transcription.* Nature, 2007. **447**(7143): p. 407-12.

123. Herman, J.G. and S.B. Baylin, *Gene silencing in cancer in association with promoter hypermethylation.* N Engl J Med, 2003. **349**(21): p. 2042-54.

124. Jin, Z., et al., *Promoter hypermethylation of CDH13 is a common, early event in human esophageal adenocarcinogenesis and correlates with clinical risk factors.* Int J Cancer, 2008. **123**(10): p. 2331-6.

125. Kim, D.S., et al., *Aberrant methylation of E-cadherin and H-cadherin genes in nonsmall cell lung cancer and its relation to clinicopathologic features.* Cancer, 2007. **110**(12): p. 2785-92.

126. Oster, B., et al., *Identification and validation of highly frequent CpG island hypermethylation in colorectal adenomas and carcinomas.* Int J Cancer, 2011.

127. Chiba, T., et al., *Cell growth inhibition and gene expression induced by the histone deacetylase inhibitor, trichostatin A, on human hepatoma cells.* Oncology, 2004. **66**(6): p. 481-91.

128. Hellebrekers, D.M., et al., *Epigenetic regulation of tumor endothelial cell anergy: silencing of intercellular adhesion molecule-1 by histone modifications.* Cancer Res, 2006. **66**(22): p. 10770-7.

129. Webb, D.J., C.M. Brown, and A.F. Horwitz, *Illuminating adhesion complexes in migrating cells: moving toward a bright future.* Curr Opin Cell Biol, 2003. **15**(5): p. 614-20.

130. Wimmer, R., et al., *Angiogenic sprouting requires the fine tuning of endothelial cell cohesion by the Raf-1/Rok-alpha complex.* Dev Cell, 2012. **22**(1): p. 158-71.

131. Bakolitsa, C., et al., *Structural basis for vinculin activation at sites of cell adhesion.* Nature, 2004. **430**(6999): p. 583-6.

132. Chervin-Petinot, A., et al., *Epithelial protein lost in neoplasm (EPLIN) interacts with alpha-catenin and actin filaments in endothelial cells and stabilizes vascular capillary network in vitro.* J Biol Chem, 2012. **287**(10): p. 7556-72.

133. Fonar, Y. and D. Frank, *FAK and WNT signaling: the meeting of two pathways in cancer and development.* Anticancer Agents Med Chem, 2011. **11**(7): p. 600-6.

134. Pandur, P., D. Maurus, and M. Kuhl, *Increasingly complex: new players enter the Wnt signaling network.* Bioessays, 2002. **24**(10): p. 881-4.

135. Chen, X.L., et al., *VEGF-induced vascular permeability is mediated by FAK.* Dev Cell, 2012. **22**(1): p. 146-57.

14 ABBREVIATIONS

4EBP	Eukaryotic initiation factor (eIF) 4E-binding protein 1
BAD	B-cell-lymphoma-2-antagonist of cell death
Cdh13	Cadherin 13
C-TAK1	Protein kinase Cdc25 C-associated kinase 1
C-terminus	Carboxy-terminus
DMEM	Dulbecco's modified eagle medium
EC	Extracellular cadherin
ECIS	Electric cell-substrate impedance sensing
ECM	Extracellular matrix
EIF4E	Eukaryotic translation-initiation factor 4E
F-actin	Filamentous actin
FACS	Fluorescence-activated cell sorting
FAK	Focal adhesion kinase
FCS	Fetal calf serum
FDCP	Factor-Dependent Cell Progenitor
FGF	Fibroblast growth factor
FITC	Fluoresceinisothiocyanat
FKBP12	12-kDa FK506-binding protein
FRAP	FKBP12-rapamcyin-associated protein
GbL	G-protein b-subunit like protein
HIF	Hypoxia inducible transcription factor
HP1	Heterochromatin protein 1
HUVEC	Human umbilical vein endothelial cells
IRES	Internal ribosomal entry site
IRS-1	Insulin receptor substrate 1
JAK-STAT	Janus kinase and signal transducer and activator of transcription
JAM2	Junctional adhesion molecule 2
MAEC	Mouse aortic endothelial cells
mLST8	Mammalian lethal with SEC13 protein 8
mSIN1	Mammalian stress-activated map kinase-interacting protein 1
mTOR	Mammalian target of rapamycin

mTORC2	mTOR complex 1
mTRORC1	mTOR complex
NFATc4	Nuclear factor of activated T-cells cytoplasmic 4
N-terminus	Amino-terminus
o/n	Overnight
PDK1	Phosphoinositide-dependent kinase 1
PI	Propidium iodide
PI3K	Phosphatidylinositol 3-kinase
PIM1	Proviral integration site for moloney leukemia virus 1
PKB	Protein kinase B
PRAS40	Pro-rich Akt substrate
RAFT	Rapamycin and FKBP12 target
RAPT	Rapamycin target
Raptor	Regulatory associated protein of mTOR
Rictor	Rapamycin-insensitive companion of mTOR
p70 S6 kinase	p70 ribosomal S6 protein kinase 1
SEP	Sirolimus effector protein
SOCS	Suppressor of cytokine signalling
SRR	Serine rich region
STAT5	Signal transducer and activator of transcription 5
TOR	Target of rapamycin
TSC1	Tuberous sclerosis complex 1
TSC2	Tuberous sclerosis complex 2
VE-cadherin	Vascular endothelial cadherin
VEGF	Vascular endothelial growth factor
WNT	Wingless-int

15 CURRICULUM VITAE

Personal Details

Name:	Walpen
First Name:	Thomas
Adress:	Division of Internal Medicine University Hospital Zürich Gloriastrasse 30 8091 Zürich
Date of Birth:	August 25th 1980
Place of Birth:	Naters
Nationality:	Swiss

Postgraduate Education

2007 - 2012	Phd Thesis in the group of Prof. Edouard Battegay, Division of Internal Medicine, University Hospital Zürich, Switzerland and the Departement of Biomedical Research, University Hospital Basel, Switzerland Title: PIM1 kinase in endothelial adhesion and proliferation
2007	Introductory course in laboratory animal science (LTK Modul 1)

University Education

2004 - 2005	Diploma thesis in the group of Ruth Chiquet-Ehrismann, Friedrich Miescher Institute, Basel, Switzerland, Thesis title: Promoter analysis of the tenascin-W gene.

2003 - 2004 Diplomstudium in molecular biology, Biozentrum, University of Basel, Switzerland

Major Subjects : Cell biology und Neurobiology
Biochemistry
Microbiology und Immunology
Biophysics und Structural Biology
Elective course : Medical Microbiology

2000 - 2003 Vordiplomsstudium, Biozentrum, University of Basel, Switzerland

Education

1995 - 2000 Eidgenössische Matura Typus B (Latein), Kollegium Spiritus Sanctus in Brig, Switzerland

1988 - 1995 Primary and secondary school in Naters, Switzerland

Publications

Thomas Walpen, Martin Peier, Elvira Haas, Ina Kalus, Jürg Schwaller, Edouard Battegay, Rok Humar. Loss of *Pim1* imposes a hyperadhesive phenotype on endothelial cells. Cellular Physiology and Biochemistry. In press.

Martin Peier, Thomas Walpen, Gerhard Christofori, Edouard Battegay, Rok Humar. Sprouty2 expression controls endothelial monolayer integrity and quiescence. Submitted to Angiogenesis 2012. In revision.

Thomas Walpen, Ina Kalus, Martin Peier, Jürg Schwaller, Edouard Battegay, Rok Humar. PIM1 nuclear translocation confers rapamycin insensitivity on endothelial cells and promotes cell proliferation. In preparation